Hydrological and landscape controls on dissolved organic matter dynamics in European wetlands

Chiara Santinelli [1*], Carlos Rochera[2*], Claudia Tropea[1], Jonas Schiller[3], Mihai Adamescu[4], Raquel Ambrosio[5], Katrin Attermeyer[6], Giancarlo Bachi[1], Nina Bègue[5], Peer Bork[3], Martynas Bučas[7], Adrian Burada[8], Miguel Cabrera-Brufau[9], Alba Camacho-Santamans[9], Rafael Carballeira[2], Marco Carloni[1], Lamara Cavalcante[10], Constantin Cazacu[4], Giovanni Checcucci[1], Pedro J. Coelho[10], Valentin Dinu[4], Valtere Evangelista[1], Jonas Gintauskas[7], Relu Giuca[4], Anis Guelmami[5], Mirco Guerrazzi[1], Samuel Hilaire[5], Leonard I. Wassenaar[6], Marija Kataržytė[7], Ana I. Lillebø[10], Raquel Lizán[2], Camille Minaudo[9], Benjamin Misteli[6], Montes-Pérez J.[9], Morant D.[2], Biel Obrador[9], Bruna R.F. Oliveira[10], Vitor F. Oliveira,[10], Marta Pedrón[2], Jolita Petkuvienė[7], Antonio Picazo[2], Tudor Racoviceanu[4], Sara Ribeiro[10], Michael Ronse[5], Ana I. Sousa[10], Wouter Suykerbuyk[11], Edvinas Tiškus[7], Diana Vaičiūtė[7], Silvia Valsecchi[1], Marinka van Puijenbroek[11], Daniel von Schiller[9], Mourine J. Yegon[6], Camacho Antonio[2]

[1]Consiglio Nazionale delle Ricerche (CNR), Istituto di Biofisica, Via Moruzzi 1, 56124 Pisa (PI), Italy
[2]University of Valencia C/Catedràtic José Beltran, 2, 46980, Paterna, Spain
[3]EMBL, Heidelberg Meyerhofstr. 1, 69117, Heidelberg, Germany
[4]University of Bucharest spl. Independentei, 91 - 95, 050095, Bucharest, Romania
[5]Tour du Valat Le Sambuc, 13200, Arles, France
[6]WasserCluster Lunz - Biologische Station Dr. Carl Kupelwieser Promenade 5, 3293, Lunz am See, Austria
[7]Marine Research Institute, Klaipėda University Universiteto ave. 17, 92294, Klaipėda, Lithuania
[8]Danube Delta National Institute for Research and Development Str. Babadag, nr. 165, 820112, Tulcea, Romania
[9]Departament de Biologia Evolutiva, Ecologia i Ciències Ambientals, Universitat de Barcelona (UB) Diagonal 643, 08028, Barcelona, Spain
[10]University of Aveiro Campus de Santiago, 3810-193, Aveiro, Portugal
[11]Wageningen Marine Research Korringaweg 7 , 4401 NT, Yerseke, Netherlands

* These authors contributed equally to the paper

Corresponding authors: Chiara Santinelli (chiara.santinelli@cnr.it), Carlos Rochera (carlos.rochera@uv.es), Antonio Camacho (antonio.camacho@uv.es)

This manuscript is a non peer reviewed preprint submitted to EarthArXiv. It was submitted to Biogeoscience for peer review on 28/12/2025.

Abstract. Dissolved organic matter (DOM) is a key component in aquatic ecosystems, representing the main source of energy for microbial metabolism and playing a crucial role in C sequestration and export. Its optical properties (absorption and fluorescence) provide integrated information on its quality (average molecular weight and aromaticity degree, main sources, presence of protein like and humic-like substances). This paper provides an assessment of the impact of catchment characteristics, seasonality and ecological conditions (altered, restored, well-preserved) on DOM dynamics across six European coastal wetlands of contrasting ecological types. DOM concentration and optical properties show inter-wetland differences, with the highest concentrations of DOC in evaporation-driven Mediterranean systems and the lowest ones in Atlantic daily tidally-flushed wetlands. Water-isotope data and optical properties indicate that hydrological confinement, water-residence time and catchment inputs primarily control DOM accumulation and composition, while microbial and photochemical processing modulate its removal within sites. Wetland restoration effects on DOM are evident where hydrological modification reduced eutrophic stress. In evaporation-driven Mediterranean systems, the recovery of more natural flooding regimes limits connectivity and promotes the accumulation of recalcitrant DOM, potentially contributing to long-term carbon sequestration. In tidally renewed systems, changes in DOM concentration and optical properties, potentially associated with restoration, are less evident, as the strong diel flux overcome possible changes. Because DOM biological lability is directly linked to carbon processing, these patterns suggest that future climate scenarios, characterized by enhanced evaporation, warming and hydrological connectivity, will amplify existing contrasts among wetland types and thereby influence carbon balances. This study provides the first continental-scale baseline of DOM dynamics in European coastal wetlands and highlights the value of optical properties as early-warning proxies to anticipate shifts in carbon cycling under ongoing climate and land-use change.

Keywords: Dissolved Organic Matter, Coastal wetlands, Carbon cycle, Ecological restoration, climate change

1 Introduction

Coastal wetlands are highly dynamic ecosystems at the land-sea interface, where physical, chemical and biological processes regulate the cycling of matter and energy. Despite covering less than 5 % of the Earth's surface, their high productivity and carbon-rich soil and sediments allow them to store approximately 35% of terrestrial carbon (C), highlighting their key role in global C dynamics (Garcia et al., 2022; Robertson et al., 2025). In these systems, dissolved organic matter (DOM), a complex mixture of organic compounds of both natural and anthropic origin, plays a central role in ecological and biogeochemical processes (Retelletti Brogi et al., 2015; Deininger and Frigstad, 2019; Kurek et al., 2024). DOM strongly influences water quality and microbial metabolic activities through multiple mechanisms, including: (1) binding metals and organic pollutants, especially mercury, thereby changing their bioavailability and toxicity (Chiasson-Gould et al., 2014); (2) providing an essential substrate for heterotrophic microbial growth, supporting respiration and secondary production (Hessen, 1992; Amaral et al., 2021; Yao et al., 2024); and (3) affecting water transparency and light penetration, influencing primary production of phytoplankton and aquatic plants (Häder et al, 2015). The main external inputs of DOM to wetlands include: (1) diffuse sources, like water and soil run-off following precipitation events and (2) point sources, which result from wastewater treatment plans (WWTP), according to the implementation of Water Framework Directive (WFD). Diffuse sources are the most challenging to quantify, as they depend on land use and climatic events. In the water, DOM can be produced by primary production, mainly by phytoplankton and plant, and by the degradation of terrestrial plants debris (Shang et al., 2018; Voss et al., 2021). Removal processes are mainly driven by microbial degradation, which converts the labile fraction of DOM into inorganic nutrients, CO_2 and microbial biomass, as well as photodegradation, which turns DOM into oxidated compounds and CO_2 (Vähätalo and Wetzel, 2008; Cory et al., 2015). The balance between these processes is strongly influenced by environmental variables but also by the ecological conditions of wetlands (Fukushima et al., 1996; Wen et al., 2022). Hydrologic connectivity regulates the input of allochthonous DOM and controls the salinity gradient, which can also affect DOM concentration and quality through aggregation and flocculation (Asmala et al., 2014). In tidally influenced coastal wetlands, tidal flushing regulates both the concentration and composition of DOM by diluting freshwater inputs and enhancing mixing between terrigenous and marine organic matter.

DOM dynamics is also affected by seasonality, influencing ecological and hydrological processes at the land-sea interface (Zhang set al., 2022; Kurek et al., 2024). In the warmest months, high temperatures promote microbial removal of DOM, but also enhances the evaporation of water, resulting in DOM accumulation. Similarly, high solar irradiation has a double effect, it enhances the photosynthetic production and therefore the release of DOM in-situ, but it also increases DOM photodegradation. In autumn-winter, rainfall increases the terrigenous fraction of DOM by runoff inputs, thereby impacting microbial mineralization rates (Chupakov et al., 2024). The seasonal growth and decay cycle of vegetation leads to a cyclic input of DOM from plant litter and root exudates (Singh et al., 2014). Importantly, these seasonal drivers not only shape DOM quantity and quality within the wetland, but also control the amount and composition of DOM exported to adjacent coastal waters.

When in good ecological status, wetlands provide essential (a) ecosystem services (e.g. C storage) (Mitsch et al., 2015), (b) provisioning services (e.g. natural resources for human consumption, energy production, and freshwater supply), (c) cultural services, namely with aesthetic, recreational and inspirational value (e.g. fishing, tourism). Nowadys, the overexploitation of these services, especially the provisioning services, has led to the degradation and loss of wetland ecosystems (Van Asselen et al., 2013; Häder & Barnes, 2019). Over the past centuries, a significant proportion of the world's wetlands has been fragmented, degraded and lost due to human activities, with the rate of loss increasing sharply in recent decades (Fluet-Chouinard et al., 2023). In response to habitat degradation, several policies have prioritized wetland restoration, such as the EU Nature Restoration Regulation (Regulation (EU) 2024/1991), which aims at reversing biodiversity loss and mitigate the impacts of climatic change. Restoration efforts include a variety of actions, from passive regeneration to active management of sediment, water, vegetation and salinity (Williams, 2001; Herbert et al., 2015; Elsey-Quirk et al., 2019; Misteli et al. 2025). There is a clear lack of empirical evidence on how restoration influences DOM concentration and quality, as well as on its role in C fluxes.

The main goal of this study is to provide a novel and comprehensive assessment of DOM dynamics across European coastal wetlands. This paper reports the first seasonal data on DOM concentration and optical properties (absorption and fluorescence) at two Mediterranean coastal marshes and wetlands, characterized by temporary hydrology and intensive artificial water management (Morant et al., 2020); two Atlantic intertidal ecosystems, strongly influenced by tidal dynamics and salinity gradients; one large lagoon and one river delta, which act as transition and buffer zones between major river basins and the marine environment.

In this study we investigated the impact of catchment characteristics, seasonality and ecological conditions (altered, restored, well-preserved) on DOM dynamics. The hypotheses we want to test are: (1) DOM dynamics (in terms of concentration and quality, assessed through optical properties) is driven by catchment characteristics and hydrological regimes, leading to differences across the six wetlands and influencing the role of DOM in C storage; 2) restoration actions, which are wetland-specific, may influence DOM concentration and quality; (3) seasonal variability can be an important driver of DOM dynamics.

2. Material and methods

2.1. Study site and sampling design

The study was conducted at six European coastal wetlands distributed along a broad geographic gradient, from Atlantic tidal systems to continental and Mediterranean marshes (Oliveira et al, under review), which showed contrasting hydrological regimes and restoration contexts (Fig. 1). Ria de Aveiro (Portugal) and the Dutch Delta (Netherlands) are tidal wetlands dominated by seagrass beds and saltmarshes, respectively, both have experienced physical alterations due to erosion and coastal protection structures and are currently under restoration through seagrass transplantation and dike removal. Further east, the Danube Delta (Romania) and the Curonian Lagoon (Lithuania) represent more permanent freshwater systems,

formerly affected by agricultural conversion and eutrophication, respectively. Here, restoration includes hydro-morphological recovery, vegetation management, and sediment remediation. In the Mediterranean region, Camargue (France) and Marjal dels Moros (Spain) are shallow freshwater to brackish marshes historically impacted by hydrological modification, rice cultivation, and freshwater or wastewater intrusion; both are being restored through actions aimed at reestablishing the natural hydrological regime (Oliveira et al., under review).

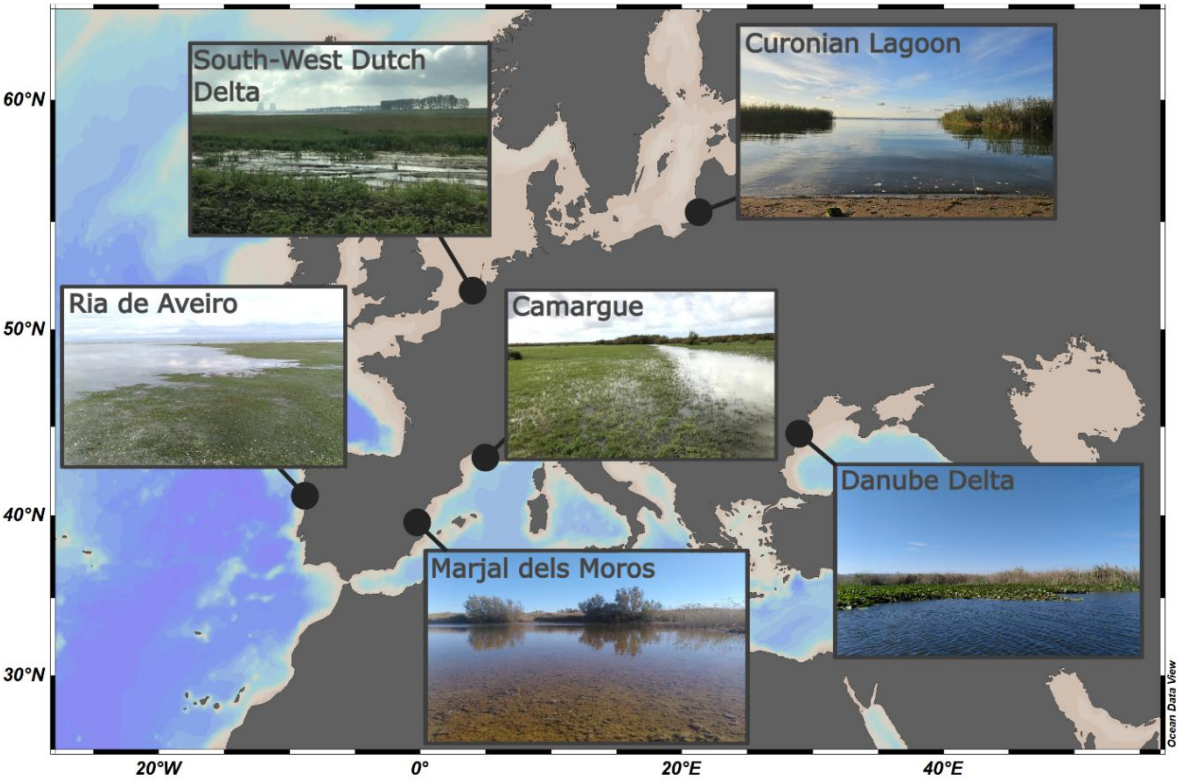

Figure 1: Map of the six European coastal wetlands studied in the RESTORE4Cs project in 2024

To capture the full range of conditions, influencing DOM dynamics across different conservation and hydrological scenarios, these six wetlands, considered as case pilots, were studied (Fig. 1 and Table 1). At each case pilot, we selected 6 subsites, characterized by 3 different ecological conditions: altered (A), restored (R), and well-preserved (P). For each condition, 2 subsites were selected. The well-preserved subsites correspond to the reference or near-natural conditions that the restored areas aim to recover, whereas the altered subsites represent the most impacted area of each wetland. In the Danube Delta, one altered subsite corresponded to a crop field and therefore lacked surface water for sampling. At the Marjal dels Moros, one well-preserved site was completely dry in autumn and summer. At each subsite, samples were collected at 3 locations, randomly selected, in order to cover the variability within the subsite.

Table 1 summarizes the main features of each wetland, including alteration type and specific restoration measures. Sampling was carried out during the four seasons to cover the different hydrological and meteorological conditions, namely: Autumn (September - October 2023), Winter (February - March 2024), Spring (May 2024) and Summer (July - August 2024).

We therefore collected 18 samples at each case pilot in each season for a total of 432 water samples. In Ria de Aveiro, samples were collected during high tide, whereas in Dutch Delta, due to logistical constrain, samples were collected during the low tide, in ponds and creeks with standing still water, it is therefore not possible to gain any information on DOM dynamics in the water column when a salt marsh is flooded.

Site ID	Country	Wetland Name	Wetland Type	Dominant Vegetation	Soil Type	Altered Site – Alteration Type	Restored Site – Restoration Type
VA	Spain	Marjal dels Moros	Brackish marshes	Halophytes, aquatic plants	Saline soils	Hydrological, trophic, or morphological change	Soil, morphology, and vegetation recovery actions
RI	Portugal	Ria de Aveiro	Intertidal seagrass	*Zostera noltei, Spartina maritima, Juncus maritimus*	Mud, sand	Erosion, stomping, bioturbation, bait digging	Vegetation and physical protection; passive restoration (natural regeneration) and active transplantation
DU	Netherlands	South-West Dutch Delta	Intertidal salt marshes	Salt marsh vegetation	Silt, mud, sandbanks	Stone breakwaters or wooden poles to reduce hydrodynamics	Management realignment Unintended restoration after dike failure
DA	Romania	Danube Delta	Freshwater	Phragmites australis, submerged/floating vegetation	Peaty/floodplain soils	Agricultural conversion of wetlands (dryland for crops/pasture)	Hydrological and morphological restoration
CA	France	Camargue	Freshwater marshes and ponds	Reed beds, halophytes	Gleysols, fluvisols	Hydrological change (used for rice growing ~30 years)	Soil, hydrology, vegetation, morphological reconstruction (former rice fields)
CU	Lithuania	Curonian Lagoon	Brackish coastal lagoon	Submerged vegetation	Muddy and sandy	Accumulated mud, reduced vegetation	Reduced mud, increased submerged vegetation coverage

Table 1. Main characteristics, alteration types, and restoration actions of the six European coastal wetlands studied.

2.2. Sampling and measure of in situ physicochemical parameters

Water column depth, temperature, conductivity, and pH were measured in situ using multiparametric probes. Surface water was collected using 5 L acid-washed food-grade PET bottles and stored in a cooler with ice packs until processing, which occurred within few hours from the sampling.

The collected water was used for the determination of dissolved and particulate nutrients, chlorophyll-a, bacterial abundance, water isotopes, Dissolved Organic Carbon (DOC), Chromophoric (CDOM) and Fluorescent (FDOM) DOM.

For the quantification of dissolved inorganic nutrients, water was filtered through pre-combusted (450 °C, 5 h) Whatman GF/F filters (47 mm diameter, 0.7 µm pore size) using a home-made peristaltic pump. The filtrate was distributed into three 20 mL acid-washed PET vials for the determination of PO_4^{3-}, NH_4^+, NO_x- (NO_2 + NO_3), Total Dissolved Phosphorous (TDP) and Total Dissolved Nitrogen (TDN). The two filters were dried and weighted for the quantification of suspended particulate matter (SPM) and then stored at -20°C to measure the concentration of Total Particulate Phosphorus (TPP) and Total Particulate Nitrogen (TPN).

A second set of GF/F glass fiber filters was used for chlorophyll-a analyses. After filtration, the filters were immediately frozen and stored in the dark until extraction and analyses.

For bacterial abundance, a homogenized subsample was taken from the unfiltered water used for the other analyses (e.g., nutrients, DOC). A 15 mL centrifuge tube was filled with unfiltered water and fixed with a PBS-buffered solution of paraformaldehyde : glutaraldehyde at final concentrations of 1% and 0.05% w/v, respectively (Rochera et al., 2024).

Samples for water isotopes were filtered into 20 ml glass vials through a 0.2µm Sterivex filter (PVDF, SVGV010RS) by using a home-made peristaltic pump.

Samples for DOC, CDOM and FDOM were filtered into 60 ml polycarbonate Nalgene bottles through a 0.2µm Sterivex filter (PVDF, SVGV010RS) by using a home-made peristaltic pump. Samples were stored in the dark and at 4°C until the analyses, carried out within 2 weeks from the sampling.

2.3. Nutrients, chlorophyll-a, water isotopes and bacterial abundance

To assess trophic status and nutrient availability, dissolved inorganic nutrient concentrations (PO_4^{3-}, NH_4^+, NO_x^-, TDN, TDP) were quantified using an automated continuous flow analyzer (Skalar San++), following Skalar standard methods aligned with APHA protocols (4500-N, 4500-P). For TPP and TPN, filters were digested with sulfuric acid (H_2SO_4) to extract particulate nutrients into soluble forms. After digestion, samples were neutralized and analyzed under the same continuous flow system (as orthophosphate and TDN, respectively). Detection limits and analytical precision adhered to manufacturer specifications, with quality control ensured through calibration curves and blanks. Parallel digestions of certified reference material NCS DC 73017 (Stream Sediment) were performed to validate the digestion of filters, with recovery efficiencies of 86 ± 13% for P and 96 ± 16% for N (n=10). Concentrations of TPP and TPN were calculated considering the volume of water that passed through each filter.

Chlorophyll-a (Chl-a) concentrations were determined spectrophotometrically, following the procedure by (Lorenzen, 1967). The δ^2H and $\delta^{18}O$ isotopic composition of water samples was analyzed using a Picarro L2130-i cavity ring-down spectroscopy (CRDS) analyzer (Picarro Inc., Santa Clara, CA, USA), calibrated to the VSMOW-SLAP as standard (Coplen and Wassenaar, 2015). Subsequently, evaporative enrichment was assessed through the deuterium excess (d-excess), calculated as the deviation of each sample from the local meteoric water line (LMWL), which was derived from the Global Meteoric Water Line (GMWL) and adjusted using local (or regional, when unavailable) precipitation data. This parameter is a proxy for evaporation processes,

since it integrates the combined influence of hydrogen and oxygen isotopic enrichment associated with evaporative processes across sites. Accordingly, low (more negative) d-excess values indicate strong evaporation and long water residence times.

Bacterioplankton abundance was quantified with a BD FACSVerse CellAnalyzer (Becton Dickinson) flow cytometer following Rochera et al. (2024). Samples were stained with SYBR Green I (Molecular Probes) in darkness for 1 hour, and cells were detected by plotting side scatter (SSC) versus green fluorescence (FL1). The ratio between green (FL1) and red (FL4) fluorescence signals was used to separate bacterial cells from background noise. Fluorescent beads (1 μm) served as size standards, and cell concentrations were calculated from the analyzed volume. The data were collected using BD FACSuite software, and data analysis was performed with FlowJo 10.8.

2.4. Dissolved Organic Carbon (DOC)

DOC concentration was measured by a Shimadzu TOC analyzer (TOC-L) by high temperature catalytic oxidation. Samples were first acidified with HCl 2 N and sparged for 3 minutes ultrapure nitrogen in order to remove the inorganic CO_2. An aliquot (150 μL) of the sample was injected into the quartz combustion tube (T~ 680 °C) and the CO_2 produced was measured by a non-dispersive infrared detector. From 3 to 5 injections were carried out until the analytical precision was lower than 2%. Different five-point calibration curves were carried out, in the concentration range of samples, with standard solutions of potassium hydrogen phthalate following the method reported by (Santinelli et al., 2015). At the beginning and the end of each analytical day, the system blank was measured using Milli-Q water and the reliability of measurements was checked by comparison with a DOC Consensus Reference Material (CRM) (Hansell 2005).

2.5. Chromophoric Dissolved Organic Matter (CDOM) analysis

Absorbance spectra were measured from 230 to 700 nm using the UV–visible spectrophotometer (UV2600i Shimadzu) equipped with a 5 cm quartz cuvette. The spectrum of Milli-Q water was subtracted from each sample spectrum. The absorption coefficient was calculated according to the equation (1):

$$a_\lambda = (2.303 \cdot A_\lambda) / L \quad (1)$$

where A is the absorbance and L is the optical path length (in meters).

The spectral slope (S) of the absorption curve was obtained through a non-linear fit using the equation (2):

$$a_\lambda = a_{\lambda_0} \cdot e^{-S \cdot (\lambda - \lambda_0)} \quad (2)$$

where λ_0 is the initial wavelength of the selected range and a_{λ_0} is the absorption coefficient at λ_0. The absorption coefficient at 254 nm (a_{254}) and the spectral slope between 275 and 295 nm ($S_{275\text{-}295}$) were calculated from the absorption spectra by using the ASFit tool (Omanović et al., 2019). a_{254} is used to have semi-quantitative information on CDOM, since primary CDOM absorption is caused by conjugated systems having the absorption peak near 254 nm (Weishaar et al., 2003; Del Vecchio and

Blough, 2004). $S_{275-295}$ is inversely correlated with average molecular weight and aromaticity degree of DOM pool (Helms et al., 2008) and can give information of the main sources of DOM, since it can be also related to the percentage of terrestrial DOC (Fichot and Benner, 2012) and to the occurrence of photobleached or microbial degraded molecules (Helms et al., 2008). The Specific Ultraviolet Absorption coefficient (SUVA254) was calculated as the ratio between a_{254} and DOC concentration following (Weishaar et al., 2003).

2.6. Fluorescent DOM and PARAFAC analysis

In order to gain information on the fluorescent fraction of DOM, Excitation-Emission matrices (EEMs) were obtained by using the Aqualog spectrofluorometer (HORIBA Jobin Yvon) with a 10 x 10 mm quartz cuvette. Emission was registered between 212 and 620 nm every 3.27 nm (8 pixels) with an integration time of 5 seconds. Excitation ranged between 250 and 450 nm and was measured every 5 nm. EEMs were corrected for instrumental bias. Rayleigh and Raman scatter peaks were removed by using monotone cubic interpolation. The EEMs were elaborated using the TreatEEM software (Omanovic et al., 2023). EEMs were corrected for the inner filter effect using the following equation (3):

$$F_{corr} = F_{obs} 10^{\frac{Abs_{Ex}+Abs_{Em}}{2}} \quad (3)$$

Where F_{corr} is the inner filter effect corrected fluorescence intensity, F_{obs} is the measured fluorescence intensity, Abs_{Ex} is the absorbance at fluorescence excitation wavelength, and Abs_{Em} is the absorbance at the selected fluorescence emission wavelength. Absorbance for inner filter correction was measured by the Aqualog spectrofluorometer (HORIBA Jobin Yvon) on the same sample used for fluorescence analysis. The corrected EEMs were normalized dividing the fluorescence intensity by the Raman band of Milli-Q water integrated between 371-428 nm (λ_{Ex} = 350 nm). Fluorescence was therefore reported in Raman Units (R.U.) following (Lawaetz and Stedmon 2009).

PARAFAC was run with different groups of EEMs, using the drEEM (decomposition routines for Excitation Emission Matrices) toolbox for MATLAB software (Murphy et al. 2013), in order to investigate if there are differences in the validated components depending on the sites, the seasons and the ecological conditions. We did the following run:

1. EEMs grouped by seasons: 4 runs with 112 EEMs for autumn, 109 EEMs for winter, 113 EEMs for spring, 105 EEMs for summer;
2. EEMs grouped by sites: 6 runs with 66 EEMs for Camargue, 72 EEMs for the Curonian Lagoon, 60 EEMs for Danube Delta, 72 EEMs for Dutch Delta, 108 EEMs for Ria d'Aveiro and 61 EEMs for Marjal dels Moros;
3. EEMs grouped by impact: 3 runs with 129 EEMs for altered, 133 EEMs for well-preserved, 141 EEMs for restored.
4. One run with all the 439 EEMs measured, in order to investigate changes in the intensity of the validated components across all the samples.

The components validated by the PARAFAC run listed above only showed slight differences in the excitation and emission spectra when the EEMs were grouped by site. season, site or ecological condition suggesting a similar mixture of fluorophores

in FDOM pool across EU wetlands without a clear effect of season or ecological conditions on the fluorescent components. We therefore decided to use the 5-components model validated by using all EEMs together (run 4). The comparison with the literature was done by using the OpenFluor tool (Table S1), that compares excitation and emission spectra of the validated components with all the components present in the database and allows to match spectrally similar components by using the Tucker congruence coefficient (TCC) (Murphy et al. 2014). By comparison with the literature the 5 components were characterize as follows (Table 2):

- **Component C1** showed a peak at $\lambda_{Ex}/\lambda_{Em}$ = 255-340/440 nm, typical of highly aromatic fluorophores observed in a variety of inland waters. Several studies (Peleato et al., 2017; Wauthy et al., 2018; Yang et al., 2019; Gullian-Klanian et al., 2021; Goranov et al., 2024) related this component to humic-like substances of terrestrial origin and to degradation products of lignin.
- **Component C2** showed a peak at $\lambda_{Ex}/\lambda_{Em}$ = 250-305/430 nm, usually related to terrestrial humic-like substances. This component is frequently found in lentic waters, and it is associated with bacterial planktonic activity (Lambert et al., 2017; Marcé et al., 2021; Kurek et al., 2022; Angelotti de Ponte Rodrigues et al., 2024;).
- **Component C3** showed a peak at $\lambda_{Ex}/\lambda_{Em}$ = 275-385/495 nm, typical of fulvic -like substances, common in all the aquatic environments and representing highly processed, complex organic matter, usually of **terrestrial** and agricultural origin (Graeber et al., 2012; Zhou et al., 2019; Zhuang et al., 2021).
- **Component C4** showed a peak at $\lambda_{Ex}/\lambda_{Em}$ = 310/390 nm, corresponding to a microbial or **marine humic**-like signal. This component is commonly found in marine surface waters and is associated with microbially processed DOM (Zhou et al., 2019; Orlova et al., 2024; Ouyang et al., 2024). Peleato et al. (2017) found that this component also associated with biofiltration, supporting its microbial origin.
- **Component C5** showed a peak at $\lambda_{Ex}/\lambda_{Em}$ = 280/350 nm and was attributed to a tryptophan-like signal, representative of in-situ produced, protein-like DOM, likely linked to microbial or algal activity (Borisover et al., 2009; Peleato et al., 2016; Batista-Andrade et al., 2023; Logozzo et al., 2023).

Component	Ex_{max}/Em_{max} (nm)	Fluorescence peak	Description
C1	255-340/440	A, C	Humic-like
C2	250-305/430	A, C	Humic-like
C3	275-385/495	C	Fulvic-like
C4	310/390	M	Marine-like
C5	280/350	T	Tryptophan, protein-like

Table 2: Fluorescence peaks positions (Ex_{max}/Em_{max}) and their corresponding DOM component types reported by (Coble 1996).

These five components collectively captured the main fluorescent DOM pools present in all the studied wetlands, including both allochthonous and autochthonous sources. The sum of their intensity was therefore used as an indicator of the total fluorescence (Ftot). The percentage of each component was calculated as C_n divided by Ftot.

2.7. Statistical analyses

2.7.1 Transformation of environmental parameters

Descriptive statistics were computed for all environmental and DOM parameters. Most of the environmental variables were not normally distributed as shown in the supplementary material (Fig. S1). To reduce the weight of outliers, skewed environmental variables (TDP, TDN, TPP, TPN, Chl-a, Bacterial abundance, DOC, a_{254}, Ftot, dissolved NH_4^+, dissolved nitrous oxide (NO_x)) were $\log_{10}$ transformed (Fig. S1).

2.7.2 Variability in environmental conditions across seasonality and conservation state

To assess whether the environmental variables differed across (i) seasons and (ii) ecological conditions (altered, restored, well-preserved), the Kruskal-Wallis test was applied for each variable per wetland. The environmental variables include water temperature, salinity, concentrations of TDN, TDP, TPP, TPN, Chl-a, bacterial abundance, DOC, CDOM (a_{254}, SUVA, $S_{275-295}$), FDOM (Ftot and the percentage of each component). The resulting p-values ($-\log_{10}$ transformed) were visualized as a heatmap. A significant result ($p < 0.05$) indicates that the distribution of that environmental variable differs among groups. Thus, the heatmap summarizes which environmental parameters show significant seasonal or ecological conditions related to differences across wetlands.

2.7.3 Comparative assessment of FDOM quality across wetlands

To summarize and compare FDOM quality across sites, a Principal Component Analysis (PCA) was applied to standardized (z-score) Excitation-Emission Matrixes (EEMs) of fluorescence. Specifically, each EEM was flattened to a one-dimensional vector and subsequently centered and scaled (z-score, R scale function). Standardizing emission values across samples, rather than using raw emission intensities, that are closely linked to fluorescence intensity, focuses the analysis on differences in the shape of EEM and therefore on FDOM quality.

To quantify the relationship between EEMs and environmental conditions, Pearson correlation between the scores of principal components and environmental parameters was calculated (Pearson's correlation coefficient r).

In order to evaluate which excitation-emission wavelengths contributed most to each of the principal components, loadings were extracted. High absolute loading values indicate a strong influence of a given excitation-emission pair on a principal component.

3. Results

3.1. Environmental characteristics of wetlands

The water column depth in the studied sites ranged from few cm up to about 3 m, with some sites occasionally drying out. Deeper and more permanent waters occurred in the eastern systems (Curonian Lagoon and Danube Delta) than in the Mediterranean (Camargue and Marjal dels Moros) and Atlantic tidal sites (Ria de Aveiro and Dutch Delta).

The water temperature ranged from 1.7 to 31.0 °C and showed a seasonal trend across all wetlands (See supplementary material, Fig. S2a, all $p < 0.001$). The highest values (average > 20°C) were observed in summer in all the sites except in the Curonian Lagoon, where no difference was observed between spring and summer (Fig. S2a). The largest range in temperature was observed in the Danube Delta with average values ranging from 5.1 °C in winter to 31.0 °C in summer. The Mediterranean wetlands showed warmer and more variable conditions than the northern ones (Curonian Lagoon and, especially, the Dutch Delta). No significant difference in water temperature was observed among sub-sites within each wetland (Fig. S2c, all $p > 0.05$).

The conductivity ranged from around 0.30 to ~175.00 mS cm^{-1}, showing a marked geographic gradient (not shown). The highest average values occurred in the Mediterranean systems, particularly Marjal dels Moros (49.53 mS cm^{-1}), where salinity is mainly driven by evaporation and geochemical concentration, and to a lesser extent in Camargue (4.66 mS cm^{-1}). The tidal sites (Ria de Aveiro and Dutch Delta) showed high conductivity typical of marine waters (28.69 mS cm^{-1} and 23.65 mS cm^{-1}, respectively), whereas the Danube Delta and Curonian Lagoon remained largely freshwater (0.90 mS $cm^{-1}$and 0.39 mS cm^{-1}, respectively).

The pH averaged globally 8.3 ± 0.6 and indicated generally alkaline conditions across sites. Overall, it tended to be slightly higher in the Mediterranean than in northern wetlands, where it reflected a limited buffering capacity in both tidal systems.

The δ^2H and $\delta^{18}O$ isotopic composition of the water samples showed that median d-excess values ranked the sites along an evaporation gradient, with the most negative and variable values (−23.65 ± 9.75‰) in Marjal dels Moros (confined Mediterranean system), intermediate values in Camargue (−10.41 ± 5.02‰), Danube Delta (−8.66 ± 4.79‰), and Curonian Lagoon (−2.72 ± 2.18‰), and the least negative values in the tidally influenced Dutch Delta (−2.02 ± 0.81‰) and Ria de Aveiro (0.05 ± 2.51‰), reflecting the effect of marine mixing (supplementary material, Fig. S2b and S2d). A clear seasonal trend (all $p < 0.001$) was observed in all the wetlands, where d-excess decreased markedly in summer and increased during autumn and winter. Seasonal variability was also observed in the tidally influenced wetlands of Ria de Aveiro and Dutch Delta where water is continuously renewed (Fig. S2b).

3.2. Trophic condition and bacterioplankton abundances

The concentrations of inorganic nutrients (both dissolved and particulate) revealed marked differences largely driven by hydrological connectivity and evaporation (supplementary material, Fig. S3 and S4). Seasonality affected TPN concentration in all the wetlands (Fig. S3b), whereas no effect on TDN was observed in Dutch Delta and Curonian Lagoon (Fig. S3a). Seasonality affected TPP only in the Danube Delta ($p<0.001$), Camargue ($p < 0.01$) and to a less extent in the Ria de Aveiro ($p<0.05$) (Fig. S4b), whereas no effect on TDP was observed in Danube Delta and Camargue (Fig. S4a). Ecological conditions strongly affected ($p < 0.001$) TPN, TPP, TDP, TDN, in Marjal dels Moros, where the highest values were observed in well-preserved sites due to intense evapo-concentration of salts, (Fig. S3c-d and S4c-d).

Chlorophyll-a showed a large variability covering 6 orders of magnitude, ranging between 0.03 to 459 μg L^{-1}. It was significantly affected ($p < 0.001$) by seasonality at Dutch Delta (maximum in summer) and Danube Delta (maximum in autumn) and with a lower significance ($p < 0.01$) at the Curonian Lagoon (maximum in autumn) and Camargue ($p < 0.05$) (supplementary material, Fig. S5a). Interestingly, the Chl-a concentration was significantly affected by ecological conditions at the (i) Curonian Lagoon ($p < 0.001$), with a maximum at the altered sub-sites, (ii) Ria de Aveiro ($p < 0.001$), with a maximum in restored sub-sites and (iii) Camargue ($p < 0.01$), with a maximum in altered sites (Fig. S5c).

Bacterioplankton abundances ranged between $2.11 \cdot 10^6$ and $12.9 \cdot 10^6$ cells mL^{-1} (supplementary material, Fig. S5b-d). The highest average abundances occurred at Danube Delta in autumn and summer, in Camargue in autumn followed by Marjal dels Moros and the Curonian Lagoon, whereas the lowest abundance were observed in Ria de Aveiro in winter and spring, in Dutch Delta in winter and Camargue in spring. Bacterial abundance was significantly affected by the season at all the sites ($p < 0.001$), even if it was less significant in Marjal dels Moros ($p < 0.05$) (Fig. S5b) In the Curonian Lagoon and Marjal dels Moros the maximum was in spring. Differences associated with ecological status were only detected in Marjal dels Moros, where well-preserved sites showed the highest values. (Fig. S5d).

3.3. Dissolved organic matter dynamics

DOC, CDOM and FDOM values covered a very wide range, with clear geographical differences, encompassing the seasons and ecological conditions (Fig. 2-6). The highest values were observed in the systems strongly affected by evaporation (e.g. Marjal dels Moros and Camargue), the lowest ones in the tidally influenced sites (e.g. Ria de Aveiro and the Dutch Delta). The Curonian Lagoon and Danube Delta exhibited intermediate conditions.

Across all samples, DOC ranged between 2 and 321 mg L^{-1} (Table 3), with both the lowest values and variability in Ria de Aveiro (2-5 mg L^{-1}), Dutch Delta (2-23 mg L^{-1}) and in the Curonian Lagoon (3-14 mg L^{-1}), whereas the highest concentration and widest range (12-321 mg L^{-1}) were observed in Marjal dels Moros and Camargue (Fig. 2a, 2c and Table 3). Only three samples, collected in Marjal dels Moros during summer at one of the well-preserved sub-sites, displayed exceptionally high

values (> 250 mg L^{-1}). If these outliers are excluded, maximum DOC concentrations decreased to 177 mg/L, with values below 10 mg L^{-1} in around half of the samples.

	DOC (mgL^{-1})	**a_{254} (m^{-1})**	**$S_{275-295}$ (10^{-3} nm^{-1})**	**SUVA (L mg C $^{-1}$ m^{-1})**	**Fluorescence (R.U.)**	**Bacterial abundance (10^6cells ml^{-1})**	**DTP (mmol P/L)**	**DTN (mmol N/L)**
Camargue	28 ± 22 (2-86)	200 ± 179 (11-622)	17.3 ± 2.8 (12.6-25.2)	6.2 ± 1.9 (2.9-10.8)	11 ±10 (1-35)	5.5 ±7.4 (0.3-35)	4 ± 6 (0-26)	141 ± 98 (22-387)
Curonian Lagoon	11 ± 2 (3-14)	75 ± 18 (50-105)	17.7 ± 0.2 (13.6-21.2)	6.7 ± 1.3 (5-10)	4.4 ± 0.9 (3-6)	4.7 ± 2.6 (1.1-11)	0.9 ± 1.1 (0.3-6.4)	112 ± 102 (42-379)
Danube Delta	15 ± 10 (2-49)	68 ± 56 (15-293)	19.9 ± 2.0 (15.8-23.8)	4.8 ± 1.1 (2.9-7.0)	4.8 ± 4.6 (1-23)	13 ± 11 (0.2-38)	1.2 ± 1.4 (0.3-5.1)	122 ± 111 (20-591)
Dutch Delta	6 ± 4 (2-23)	39 ± 25 (11-127)	15.8 ± 1.4 (12.9-19.7)	6.4 ± 1.3 (3.2-9.8)	3.3 ± 2.4 (0.7-12.6)	2.6 ± 2.0 (0.3-9.7)	4.9 ± 8.2 (0.6-50)	84 ± 67 (12-329)
Ria de Aveiro	3 ± 1 (2-13)	17 ± 8 (7-48)	15.1 ± 0.2 (12.4-18.7)	6.6 ± 2.0 (0.7-10.2)	1.2 ± 0.6 (0.5-3.3)	2.1 ± 3.0 (0.2-17)	1.0 ± 0.3 (0.5-1.8)	75 ± 65 (11-384)
Marjal dels Moros	73 ± 67 (12-321)	305 ± 213 (62-984)	24.8 ± 0.5 (17.1-35.4)	4.8 ± 2.0 (1.3-14.5)	15.9 ± 8.9 (3.8-43.7)	9.4 ± 12.0 (0.8-73)	3.9 ± 18.4 (0.3-138.0)	675 ± 976 (98-7276)

Table 3. Mean ± standard deviation and ranges of the different parameters in across the 6 six coastal wetlands taking into consideration all the databased on the complete dataset.

Seasonal differences in DOC concentrations were observed in the Curonian Lagoon ($p < 0.001$), Danube Delta ($p < 0.01$), and Dutch Delta ($p < 0.01$) (Fig. 2a). Regarding ecological conditions, significant effects ($p < 0.001$) were detected at Marjal dels Moros, Camargue, and Ria de Aveiro ($p < 0.01$), though the direction and magnitude of these differences varied among sites (Fig. 2c). Intra-site variability was also observed, particularly in Marjal dels Moros, where the two well-preserved sub-sites exhibited divergent behaviors, and in the Camargue, where the altered sites displayed distinct patterns, suggesting an additional influence in DOM dynamics by local drivers beyond the ecological conditions.

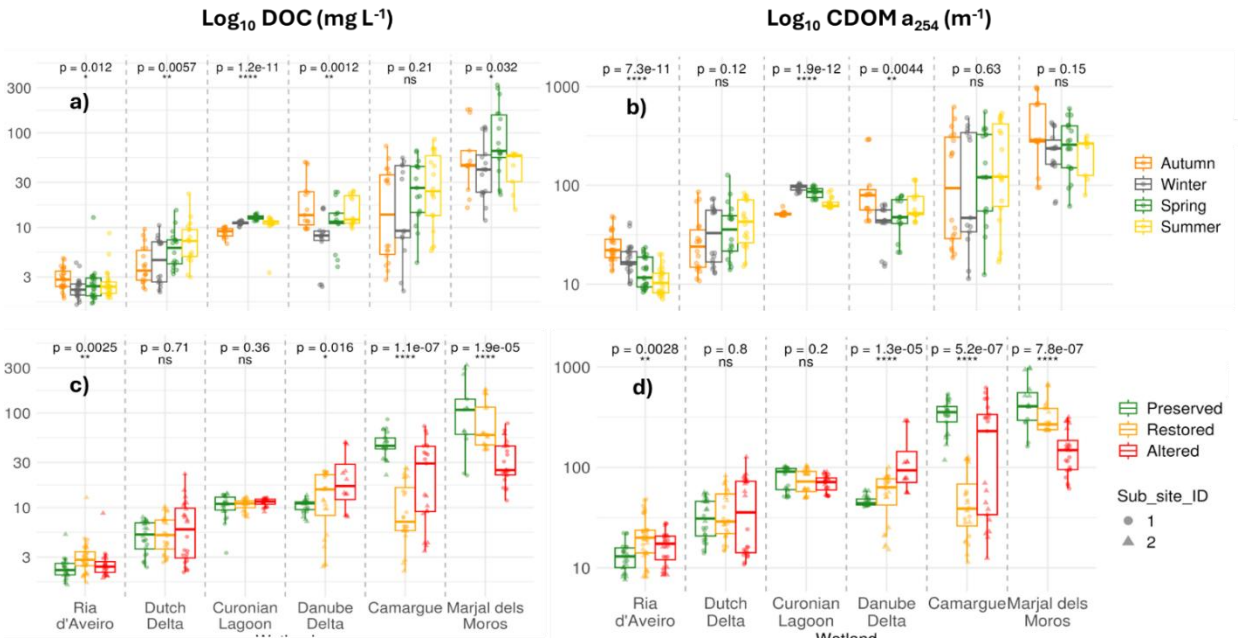

Figure 2. Boxplots on a logarithmic scale showing DOC across the six studied European coastal wetlands, grouped by season (a) and ecological conditions (c) and absorption coefficient a_{254} across the six studied European coastal wetlands, grouped by season (b) and ecological conditions (d). Significant differences were assessed using the Kruskal–Wallis test. (*p<0.001, **p<0.01, *p<0.05, ns = no significance).**

Comparison of the wetland-averaged absorbance spectra revealed differences in both absorption intensity and spectral shape (supplementary material, Fig. S6). The spatial pattern of a_{254}, closely resembled that of DOC, with the highest values and variability in Marjal dels Moros and Camargue and the lowest ones in Ria de Aveiro and the Dutch Delta. Seasonal and sub-site differences also occurred, but without modifying the overall geographical pattern (Fig. 2b and 2d). Values ranged broadly between 11 and 984 m^{-1}, although in 97% of the samples were below 490 m^{-1}. Significant seasonal differences in a_{254} were detected at the Curonian Lagoon ($p < 0.001$), Danube Delta ($p < 0.01$), and Ria de Aveiro ($p < 0.001$) (Fig. 2b). With respect to ecological conditions, a_{254} also differed significantly at Marjal dels Moros, Camargue and Danube Delta ($p < 0.001$), and to a less extent Ria de Aveiro ($p < 0.01$), although the specific patterns varied between sites (Fig. 2d).

DOM aromaticity was assessed using two complementary optical indicators: $S_{275-295}$ and specific UV absorbance (SUVA). The $S_{275-295}$ and SUVA support contrasting DOM composition and aromaticity degree across wetlands. $S_{275-295}$ ranged from 0.013 to 0.035 nm^{-1} with the highest values and variability in Marjal dels Moros and Danube Delta (Table 3), suggesting the predominance in the DOM pool of molecules with low molecular weight and aromaticity degree. This observation is further supported by SUVA, that ranged from 1.3 to 10.2 L mg C^{-1} m^{-1} and showed the lowest values in Marjal dels Moros (Table 3). Both parameters were significantly affected by season in Ria de Aveiro and the Curonian Lagoon (Fig. 3a, 3b), with a clear impact of photobleaching. The highest values of $S_{275-295}$, usually associated with photodegraded molecules (Helms et al., 2008),

were observed in Ria de Aveiro in spring-summer, when photobleaching is at its maximum (Fig. 3a). In the Curonian Lagoon, water temperature decreased from spring-summer to winter (Fig. S2) and $S_{275-295}$ increased from spring to summer, to reach a pronounced minimum in winter, suggesting a wintertime increase in DOM aromaticity and average molecular weight (Fig. 3a). This observation further indicates a clear cycle of DOM in the Curonian Lagoon with an increase in humic-like substances from summer to winter. $S_{275-295}$ showed a significant link with ecological conditions in the Marjal dels Moros and Danube Delta, indeed in both cases altered sites showed the lowest values (Fig. 3c). SUVA was significantly ($p < 0.01$) affected by the ecological conditions in Camargue and Danube Delta but not at Marjal dels Moros (Fig. 3d). By applying the Weishaar regression to our SUVA data, the estimated aromatic carbon fraction across all samples ranges between 12% and 74%, reflecting (supporting) high variability in DOM quality across the studied sites.

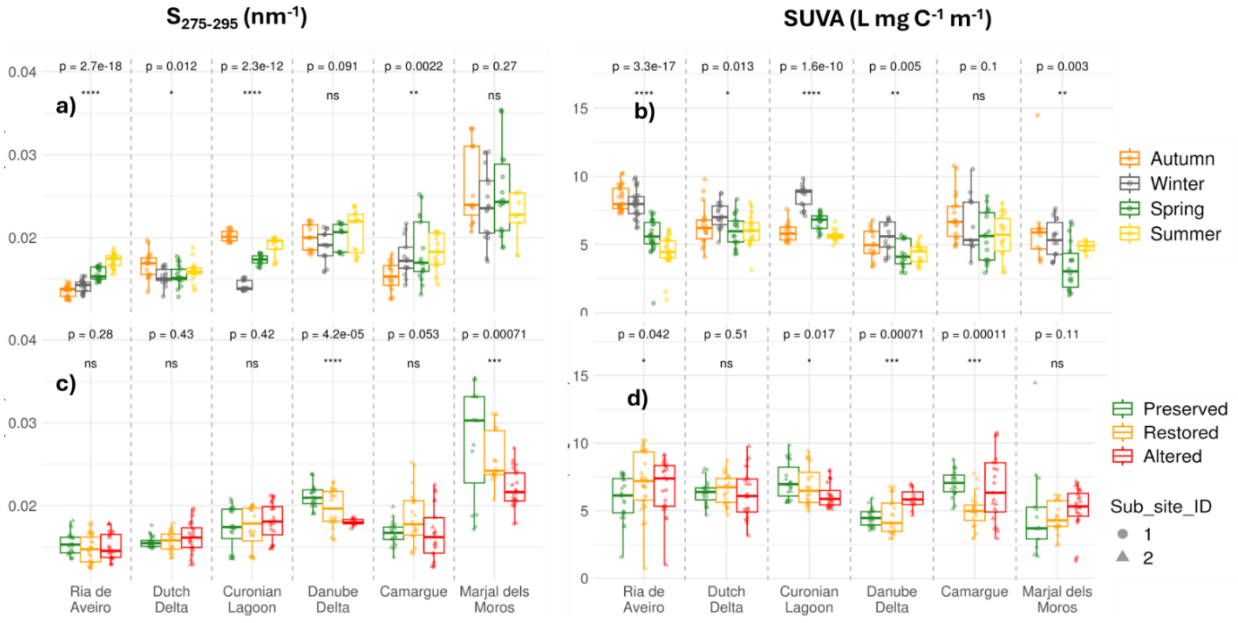

Figure 3. Boxplots of $S_{275-295}$ across the six studied European coastal wetlands, grouped by season (a) and ecological conditions (c) and SUVA across the six studied European coastal wetlands, grouped by season (b) and ecological conditions (d). Significant differences were assessed using the Kruskal–Wallis test. (*p<0.001, **p<0.01, *p<0.05, ns = no significance).**

As already observed for DOC and CDOM, the highest fluorescence intensity and variability was observed in Marjal dels Moros and Camargue (Fig. 4-6). Intermediate values, but with high variability, were also observed at Dutch and Danube Delta. The highest contribution (>80%) to fluorescence was given by humic-like and fulvic-like substances in all the sites (Fig. 4-5). In most of the samples, protein-like substances represented between 10 and 20% of the total fluorescence (Fig. 6a , 6c). Significant seasonal differences in Ftot were observed in Ria de Aveiro ($p < 0.001$), Curonian Lagoon ($p < 0.001$) and Danube Delta ($p < 0.01$) (Fig. 6b), whereas ecological conditions significantly ($p < 0.001$) affected Ftot at Camargue, Marjal dels Moros and

Danube Delta, but with different pattern (fig. 6d). In Camargue and Marjal dels Moros well-preserved sites showed the highest fluorescence, whereas Danube Delta the lowest one. Significant seasonal differences ($p < 0.01$) also affected %C1, %C2 (Fig. 4) and %C4 at all the sites (Fig. 5b, 5d).

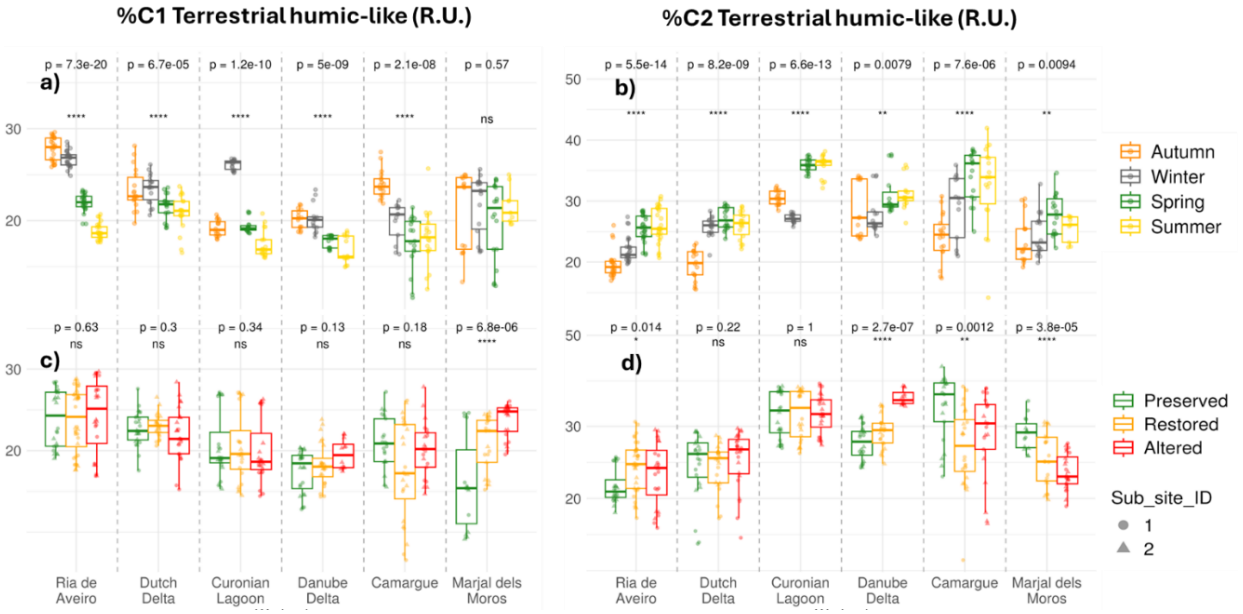

Figure 4. Boxplots of %C1 across the six studied European coastal wetlands, grouped by season (a), and ecological conditions (b) and %C2 across the six studied European coastal wetlands, grouped by season (c) and ecological conditions (d). Significant differences were assessed using the Kruskal–Wallis test. (*p<0.001, **p<0.01, *p<0.05, ns = no significance).**

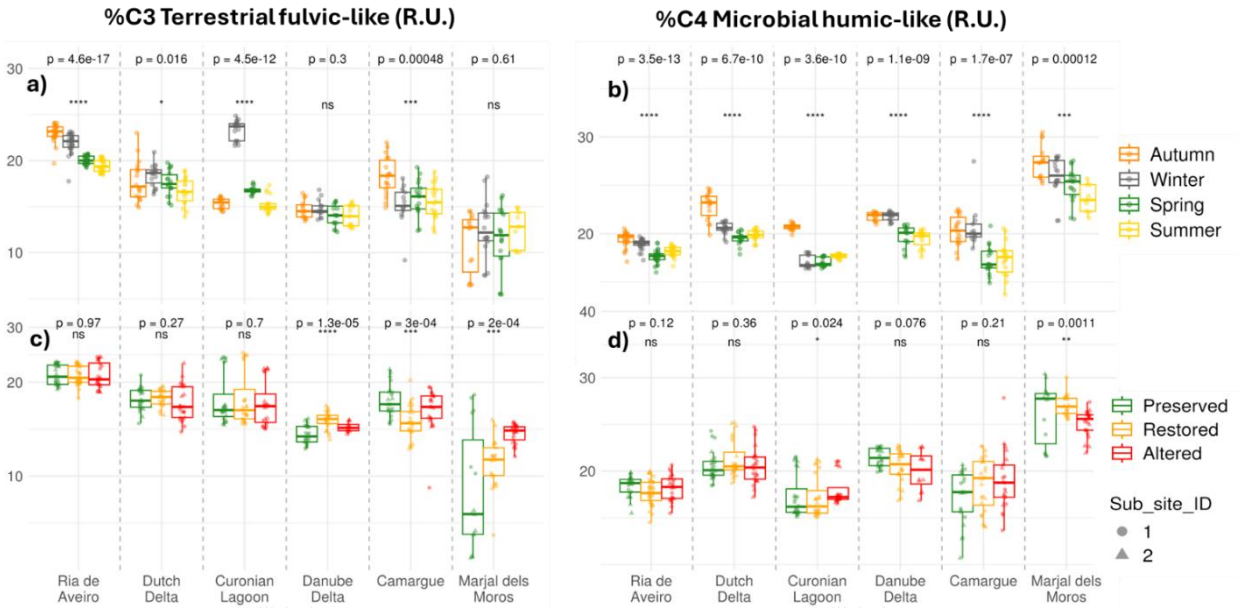

435

Figure 5. Boxplots of %C3 across the six studied European coastal wetlands, grouped by season (a), and ecological conditions (b) and %C4 across the six studied European coastal wetlands, grouped by season (c) and ecological conditions (d). Significant differences were assessed using the Kruskal–Wallis test. (*p<0.001, **p<0.01, *p<0.05, ns = no significance).**

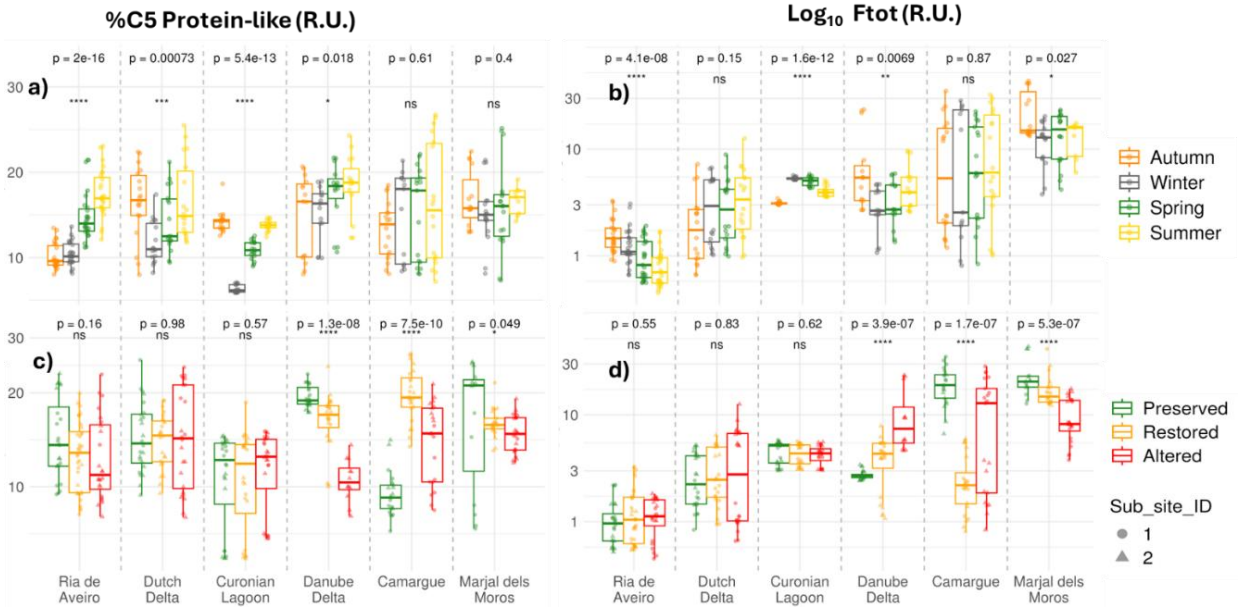

440

Figure 6. Boxplots of %C5 across the six studied European coastal wetlands, grouped by season (a), and ecological conditions (b) and on logarithmic scale of Ftot across the six studied European coastal wetlands, grouped by season (c) and ecological conditions (d). Significant differences were assessed using the Kruskal–Wallis test. (*p<0.001, **p<0.01, *p<0.05, ns = no significance).**

3.4. Linking variation in FDOM to environmental gradients

To compare the quality of FDOM across sites, seasons and ecological conditions, the excitation-emission matrix (EEM) shapes were summarized into principal components (Fig. 7). The first 2 principal components, jointly explaining 81.5% of the total variance (PC1: 60.1%, PC2: 21.4%) and exhibited a significant grouping of samples by wetland (MANOVA, Pillai's trace: $p < 0.001$, approx. $F = 90$; Fig. 7a).

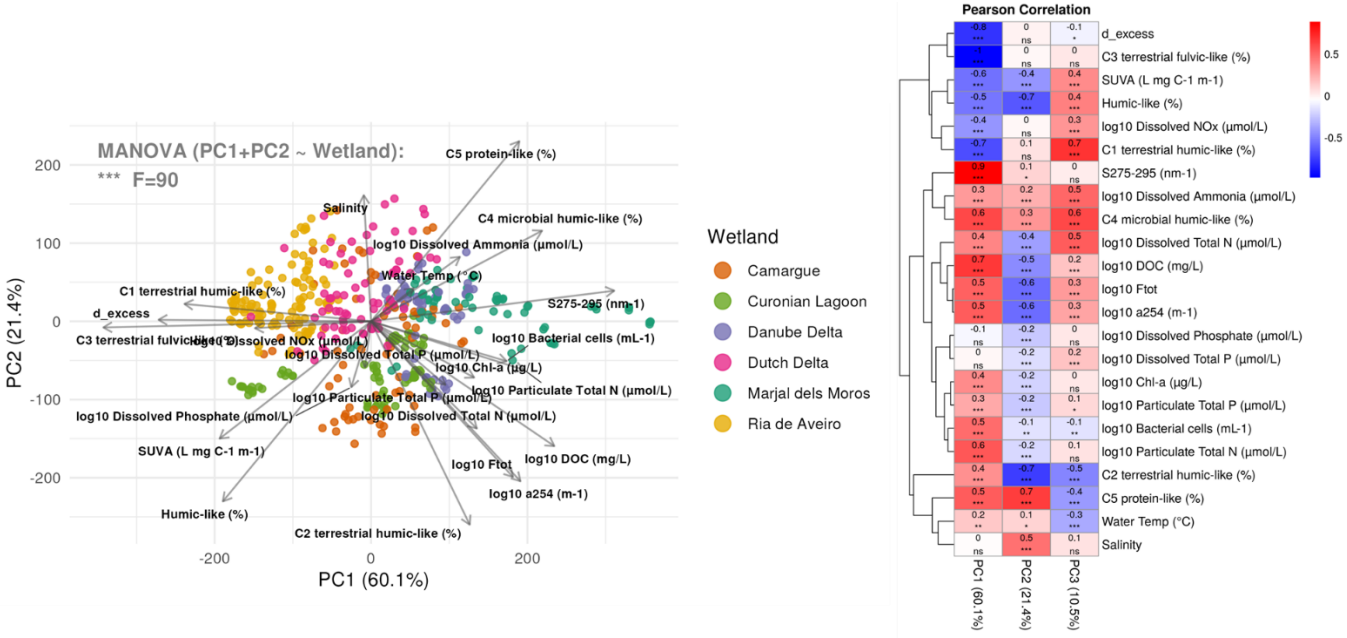

Figure 7: PCA biplot (PC1, PC2) of scaled EEMs (z-score) of for all the samples; with vectors refer representing to physical and chemical parameters (a). MANOVA test with Pillai's trace test was applied to test for significant grouping of samples in the first 2 PCs by site/Wetland (*p < 0.001) with approximated F-statistic. Pearson correlation of PC scores (PC1-PC3) with environmental variables (***p < 0.001, **p < 0.01, *p < 0.05, ns p > 0.05) (b). the dDendrogram represents hierarchical clustering using complete linkage (R pheatmap package).**

The first principal component (PC1) captures a gradient highly aligned with the third PARAFAC component of terrestrial fulvic-like substances (C3: $r = -1$, $p < 0.001$; Figure 7) and is tightly coupled to the evaporation regime (d-excess: $r = -0.8$, $p < 0.001$), separating tidally influenced wetlands (i.e. Ria de Aveiro and Dutch Delta) from confined wetlands, (i.e. Marjal dels Moros and Camargue). The latter are characterized by a steep slope between 275–295 nm in the absorption spectra ($S_{275–295}$: $r = 0.9$, $p < 0.001$), indicating lower molecular weights, and high levels of bacterial cell counts ($r = 0.5$, $p < 0.001$) and total particulate nitrogen ($r = 0.6$, $p < 0.001$).

The second principal component (PC2) is unrelated to the evaporation regime (d-excess: $r = 0$, $p > 0.05$) but captures a salinity gradient ($r = 0.5$, $p < 0.001$), positively correlated with the proportion of protein-like compounds (C5: $r = 0.7$, $p < 0.001$). This suggests an influence of seawater/freshwater mixing by tidal influences on the quality of FDOM (Fig. 7).

The third principal component (PC3), explaining additional 10.5% of the variance in EEMs, in many aspects captures contrasting DOM characteristics to PC1, however is little correlated to evaporation conditions (d-excess: $r = -0.1$, $p < 0.05$), the percentage of terrestrial fulvic-like substances (C3: $r = 0$, $p > 0.05$) and $S_{275–295}$ ($r = 0$, $p > 0.05$) (Fig. 7b). In contrast to the PC2, the variance captured by PC3 is unrelated to Salinity ($r = 0.1$, $p > 0.05$) (fig. 7). This suggests that FDOM quality varies beyond the influences of evaporation, bacterial abundance and seawater/freshwater mixing.

To test whether seasonality had an impact on the shape of the EEM at each wetland site, the distribution of different-season samples of each wetland in biplots of PC1 and PC2 is reported (Fig. 8). In 4 out of 6 wetlands, EEM profiles grouped significantly by season in the first two principal components, quantified by MANOVA (Pillai's trace test). The grouping by seasonality was most pronounced for the Curonian Lagoon (approx. $F = 155$, $p < 0.001$), followed by Ria de Aveiro (approx. $F = 29$, $p < 0.001$), Dutch Delta (approx. $F = 9$, $p < 0.001$) and Camargue (approx. $F = 7$, $p < 0.001$). In contrast, no significant season-specific grouping in the first 2 PCs was evident in the Danube Delta and Marjal dels Moros (both $p > 0.05$; Fig. 8).

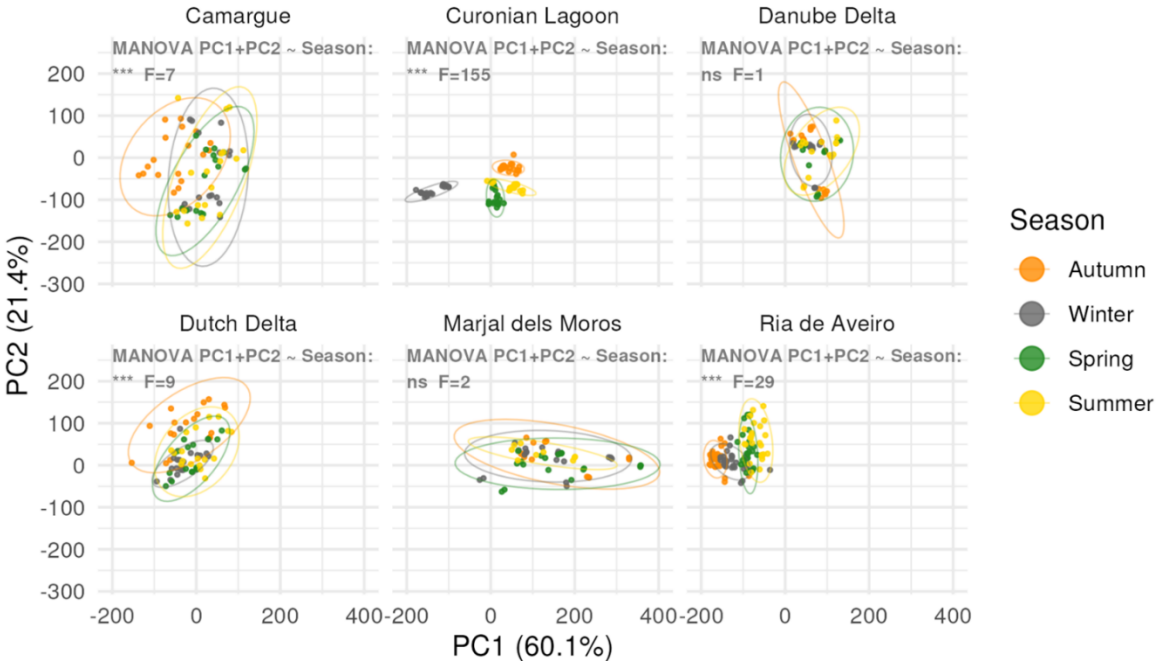

Figure 8: PCA biplot (PC1, PC2) of scaled EEMs (z-score), facetted by site. Color refers to the season at the sampling time. Ellipses indicate the spread and orientation of samples by season (confidence level = 0.95; ggplot2 R package). For each site, MANOVA test with Pillai's trace test was applied to test for significant grouping of samples in the first 2 PCs by season (*p < 0.001) with approximated F-statistic.**

Beyond seasonal grouping, we also observed a significant clustering of EEMs by ecological conditions (altered, restored, well-preserved; Fig. 9) in 4 out of 6 wetlands. Especially wetlands without seasonal grouping in the first 2 PCs, group well by ecological conditions: Danube Delta (approx. $F = 29$, $p < 0.001$) and Marjal dels Moros (approx. $F = 12$, $p < 0.001$). Aside of a seasonal grouping, samples from the Camargue (approx. $F = 14$, $p < 0.001$) and Ria de Aveiro (approx. $F = 7$, $p < 0.001$) also show a significant partitioning based on ecological conditions. Samples from the Curonian Lagoon and Dutch Delta are not grouped by ecological condition (both $p > 0.05$; Fig. 9).

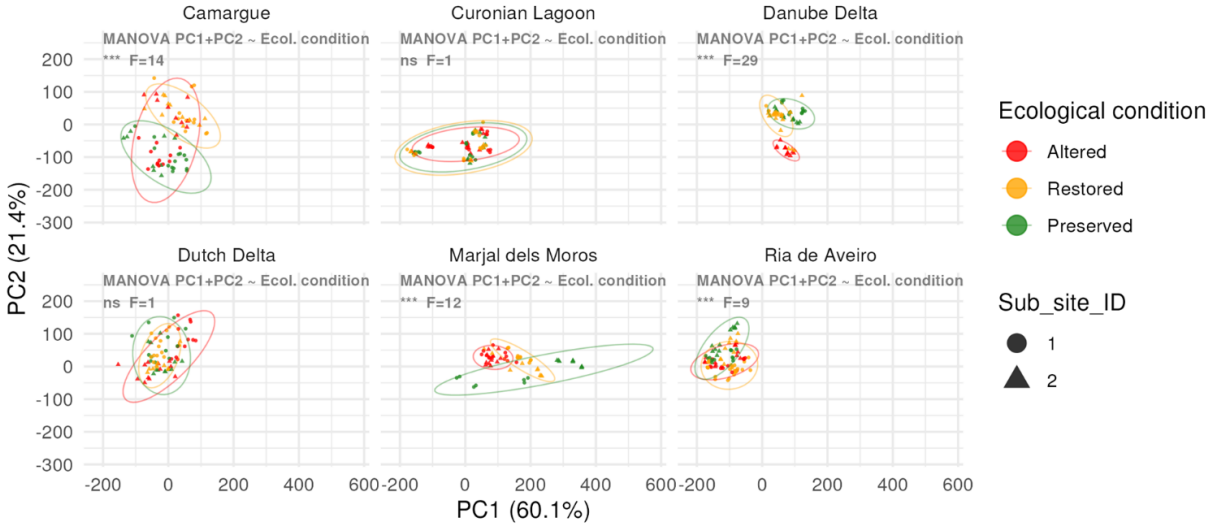

Figure 9: PCA biplot (PC1, PC2) of scaled EEMs (z-score), facetted by site. Color refers to the anthropogenic impact on the wetland. The different shapes refer to subsite 1 (circles) or 2 (triangles). Ellipses indicate the spread and orientation of samples by ecological conditions (confidence level = 0.95; ggplot2 R package). For each site, MANOVA test with Pillai's trace test was applied to test for significant grouping of samples in the first 2 PCs by impact type (*$p < 0.001$) with approximated F-statistic.**

4. Discussion

4.1. Main drivers of DOM dynamics in European Coastal wetlands

This study provides evidences of variability in DOM concentration and quality across European coastal wetlands. DOC concentration increased from the tidally influenced coastal systems (Rio de Aveiro and Dutch Delta) toward the more confined and temporary inland wetlands (Marjal dels Moros and Camargue). These differences clearly exceeded those driven by seasonality or ecological conditions, highlighting the dominant role of hydrological confinement and water renewal regime in shaping DOM dynamics at these sites. The highest DOC concentrations, observed in Marjal dels Moros and Camargue, coincide with strong evaporative stress and limited exchange with marine or freshwater sources, favoring the accumulation of

recalcitrant DOM. This observation is supported by the water-isotope data, with the strong depletion of d-excess in Marjal dels Moros and Camargue indicating intense evaporative enrichment and prolonged water residence. The intermediate d-excess values, observed in the Curonian and Danube sites, suggest transitional hydrological regimes where partial water renewal could maintain mixed DOM sources and reduce DOC concentration. Near-zero values at Ria de Aveiro and the Dutch Delta indicate the prevalence of tidal exchange and marine mixing, which is expected to dilute terrestrial DOM and to introduce in situ released or marine DOM, resulting in the lowest DOC concentrations. However, it is important to keep in mind that in the Dutch Delta, samples were collected from pools and creeks during low tide, thus representing stagnant water. Our sampling strategy does not therefore capture DOM dynamics during high tide, when the salt marsh is flooded. In these dynamic systems, during spring tide and/or stormy condition, both a decrease in DOC concentration and a change in its optical properties is expected because of the dilution of the terrestrial DOM accumulated in pools and creeks. During high tide we therefore expect values similar to those observed in Ria de Aveiro (Fig. 2). In general, the studied wetlands (excluding Ria de Aveiro) feature much higher DOC concentrations than European rivers (1.1-4.4 mg L^{-1}) (Santinelli, 2015; Thibault et al., 2019), highlighting their important role as carbon storage.

The link between hydrological regimes and DOM dynamics is further supported by CDOM optical properties, suggesting a change in DOM composition across wetlands. The highest $S_{275-295}$ values in Marjal dels Moros indicate that here the molecules with low molecular weight and low aromaticity degree dominate DOM pool, as usually reported for photobleached DOM (Helms et al., 2008; Yamashita et al., 2013; Retelletti et al., 2020; Grasset et al., 2024). In contrast, in the tidally influenced systems, the lowest $S_{275-295}$ support the predominance of molecules with high aromaticity and high-molecular-weight, with values slightly lower than those observed in the open Mediterranean Sea (Catalá et al., 2015; Galletti et al., 2019), supporting the occurrence of a fraction of terrestrial DOM even in the tidally influenced systems. This observation is further reflected in the shape of the EEMs, with Marjal dels Moros and Camargue EEMs clustering towards the confined, evaporative end, whereas Ria de Aveiro and the Dutch Delta occupy the opposite, tidally renewed extreme (Fig. 7), indicating a change in the predominance of the 5 fluorescent components across the six wetlands.

In all the six studied European wetlands, the fluorescence of the four humic-like components exceeds 80%, suggesting that the terrestrial legacy is the primary driver of DOM quality, thus potentially masking localized anthropogenic effects. However, the four humic-like components may have different origins and show distinct distribution across sites, as well as pronounced seasonality (Fig. 4 and 5). C1 and C4 components have been reported to be released by marine phytoplankton and may therefore be related to in situ release of DOM (Bachi et al., 2023). These components are also associated with microbially processed DOM (Zhou et al., 2019; Orlova et al., 2024; Ouyang et al., 2024). Interestingly, the highest dominance (20-30 %) of C4 was observed at Marjal dels Moros in all the seasons (Fig. 5b, 5d), suggesting microbial reworking as a consequence of the long resident time of DOM. Taken together C1 and C4 components represent 28-52 % of humic-like fluorescence across all the samples, indicating that in situ production can be a relevant source of DOM. If protein-like fluorescence (~20%), often associated to autochthonous DOM production (Stedmon and Markager, 2005; Bachi et al., 2023), is also taken into consideration, our data support the idea that primary production can play a complementary role compared to terrestrial inputs

of humic-like and fulvic-like substances. Macrophytes or phytoplankton might contribute to in situ DOM production during warm, productive periods when oxygen supersaturation and algal biomass peak. A significant increase in protein-like fluorescence was indeed observed in Ria de Aveiro in summer as well as in the Curonian Lagoon and in Dutch Delta in both summer and autumn (Fig. 6a, 6c).

To date, only a limited number of studies report DOM dynamics in coastal wetlands globally, and this study represents, to our knowledge, the first assessment encompassing diverse wetland habitats at European scale. When compared with DOC concentrations observed in coastal wetlands in North America, where values typically fall between 10 and 50 mg L^{-1} (Kurek et al., 2024), our data show lower average concentration in Ria de Aveiro and Dutch Delta, whereas the other sites feature comparable values. It is noteworthy that the SUVA values observed in our study (4.8–6.7 L mg C^{-1} m^{-1}), are markedly higher than those reported for the U.S. coastal wetlands (1–5 L mg C^{-1} m^{-1}) (Kurek et al., 2024), suggesting a higher proportion of aromatic and optically condensed DOM in these European coastal wetlands compared to US counterparts, likely reflecting different DOM sources. DOM in North American coastal wetlands often derive from boreal peatlands or subtropical systems (Kurek et al., 2024), whereas the European sites studied here encompass historically converted agricultural soils (e.g., Danube, Camargue) and mineral-rich estuarine sediments (e.g., Ria de Aveiro, Dutch Delta). This pattern is consistent with observations showing an important role of catchment geology and edaphic factors in driving DOM nature (Graeber et al., 2012; Lambert et al., 2014). The high aromaticity (SUVA > 4 L mg C^{-1} m^{-1}), observed in this study, likely reflects the mobilization of terrestrial carbon from alluvial and organic-rich substrates, instead of mineral soils and clearwater dominating North American systems. Differences in soils retention capacity support this observation, as mineral soils rich in clays and oxides tend to sequester aromatic compounds through adsorption, thereby lowering the SUVA of runoff water (Kalbitz et al., 2005). By contrast, the organic-rich soils dominating the European wetlands in our study lack this retaining capacity and thus favor the export of aromatic DOM. Even if there is not a clear link between aromaticity, molecular weight and biological lability, we speculate that the DOM pool in European wetlands could be more recalcitrant and therefore less prone to rapid microbial mineralization.

4.2. Seasonality

Although we identified the hydrological regime as the main driver of DOM dynamics, our data also show a clear influence of seasonality in the Curonian Lagoon and in Ria de Aveiro (Fig. 8).

In the Curonian Lagoon, temperature decreased from spring-summer to winter (Fig. S2), DOC increased from autumn to spring, whereas $S_{275\text{-}295}$ showed an increasing trend from spring to autumn, followed by a marked minimum in winter. In summer-autumn, the high $S_{275\text{-}295}$ is a clear indicator of photobleaching reducing the complexity of molecules (Retelletti et al., 2020; Yamashita et al., 2013; Helms et al., 2008). In winter, the predominance of terrestrial humic-like substances (C1 and C3) together with a minimum in the percentage of protein-like substances (C5) suggest an input of DOM from the soil as already observed in the Arno River (Retelletti et al., 2020). This observation is further supported by the minimum in $S_{275\text{-}295}$ indicating the predominance of high molecular weight and aromatic molecules in DOM pool in winter (Fig. 3a). Our data

indicate a clear temporal cycle of DOM with a change in DOM quality. If we assume that DOM quality is linked to biological lability (Romera-Castillo et al. 2011; Zheng et al. 2019; Retelletti et al., 2021), this seasonally variable composition would have an impact on C fluxes related to DOM mineralization by bacteria. Interestingly, in winter a marked minimum in bacterial abundance is also observed supporting low DOM removal rate (Fig. S5b). In contrast, in spring when DOC accumulates and the percentage of protein-like substances increases (Fig. 2a), the highest bacterial abundances are observed (Fig. S5b).

In Ria de Aveiro, the highest DOC concentrations and the highest values of a_{254} and Ftot were observed in autumn, followed by a progressive decline toward summer (Fig. 2). $S_{275-295}$ showed the opposite trend (Fig. 3a) indicating a decrease in molecular weight and aromaticity degree from autumn to summer, likely reflecting the combined effects of photobleaching (Retelletti et al., 2020; Yamashita et al., 2013; Helms et al., 2008) and microbial transformation of DOM (Kinsey et al., 2018). This observation is supported by the marked temporal decrease in terrestrial humic-like substances (C1 and C3) (Fig. 4a, Fig. 5a) and the increase in the proportion of microbial humic-like (C4) (Fig. 5b) and protein-like substances (C5) (Fig. 6a), peaking in summer. Interestingly, bacterial abundance also peaks in summer (fig. S5b), when the highest %C5 is observed. High values of bacterial abundance were also observed in autumn, suggesting an increase in DOM removal rates and bacterial growth efficiency in these periods.

There are processes at local scale that may partially mask seasonal signals, including short-term hydrological disturbances, variable water residence times, episodic terrestrial inputs, wind-driven resuspension, and site-specific differences in microbial processing and primary production. In addition, at several sites the seasonal variability of key climatic, hydrological, or biological drivers appears to be weak or non-significant, limiting the emergence of clear seasonal patterns in DOM properties and related indicators in the other studied wetlands. Under these conditions, DOM dynamics is likely dominated by persistent local controls rather than by seasonal forcing. Furthermore, while our data reveal distinct seasonal shifts in indicators like $S_{275-295}$ and protein-like fluorescence, we acknowledge that the limited temporal resolution of our sampling may not fully capture high-frequency events, such as episodic storms or transient algal blooms, which could significantly alter DOM dynamics and GHG efflux on shorter timescales.

4.3. Restoration effects

Restoration measures produced clear but contrasting signatures in DOM across the studied wetlands, with significant effects in the Danube Delta, Camargue and Marjal dels Moros (Fig. 9). In confined Mediterranean systems, such as Marjal dels Moros and the Camargue, restoration increased hydrological confinement and promoted DOM accumulation. At Marjal dels Moros, DOC and a_{254} values are consistently high at both restored and well-preserved sites, reflecting that restoration has successfully re-established natural confinement and reduced water renewal. This hydrological configuration enhances DOM accumulation through evaporation and limited dilution, typical of Mediterranean temporary wetlands under strong climatic stress. A similar pattern is observed in Camargue, although with greater variability among subsites: well-preserved subsites display the highest DOM concentrations while restored ones remain hydrologically dynamic. The occurrence of other local processes such as the

presence of caws can also explain the high values observed, hindering a clear assessment of restoration effects on DOM concentration and quality. In the Danube Delta, restoration alleviated nutrient enrichment and resulted in lower DOC concentrations than in the altered subsites, although values did not reach the baseline levels observed in well-preserved subsites. In the Curonian Lagoon, restoration effects are less evident since the strong seasonal signature of DOM dynamics likely precluded the detection of any potential restoration effect.

In the Atlantic tidally flushed wetlands, frequent marine exchange overrides local restoration effects, resulting in very low (Ria de 'Aveiro) or no significant (Dutch Delta) effect of ecological conditions. Notably, marked intra-site variability was observed, particularly in Marjal dels Moros, where the two well-preserved sub-sites exhibited divergent behaviors, and in the Camargue, where the altered sites also displayed distinct patterns. This variability suggests that local drivers, beyond broad ecological conditions, exert an additional influence on DOM dynamics.

Because DOM dynamics are tightly linked to hydrological connectivity, restoration outcomes depend on how water exchange interacts with site-specific biogeochemical processes. In Mediterranean water stressed sites, moderate adjustments in water renewal may help prevent excessive oxygen depletion while maintaining high carbon retention, although potential effects on redox balance and greenhouse gas emissions must be considered. In contrast, in tidally flushed systems, frequent water renewal hinders organic carbon accumulation, and interventions aimed at enhancing organic matter retention may conflict with natural ecosystem functioning or promote methane emissions.

Overall, our results demonstrate that DOM is a crucial variable, which should be taken into consideration in sustainable restoration strategies; even if its response needs to be considered on a case-by-case basis, since it is strongly dependent on site-specific features.

4.4. Implications for Carbon cycle

Our results highlight the strong potential of wetlands for carbon storage in the form of DOM. DOM in wetlands may have different external sources or can be released by plants and phytoplankton. DOM sustains heterotrophic metabolism and is respired to CO_2 or CH_4, or transformed into biomass. The fraction that is quickly removed and respired or transformed into biomass is defined as labile (Hansell 2013) and may represent an important source of carbon to the atmosphere. A major fraction, defined as recalcitrant, escapes the rapid microbial removal and in the oceans may accumulate for months to several millennia (Hansell 2013), playing a key role in carbon sequestration and export (Butturini et al., 2022; Corrales-González et al., 2025). Understanding the factors that determine the persistence of DOM in natural waters is crucial for our understanding of the role of DOM in the global C cycle. The biological lability is therefore the most important factor determining the role of DOM in the C cycle and in C fluxes.

In confined Mediterranean wetlands, prolonged residence time together with the intense solar irradiation led to the mineralization of the biologically labile fraction and/or its transformation into more refractory, optically condensed forms enhancing the overall recalcitrance of the remaining DOM pool (Corrales-González et al., 2025). This process could therefore

have a dual effect consisting of stimulating CO_2 release while promoting the persistence of photobleached molecules, representing a balance between short-term C loss and long-term C stabilization within the dissolved pool. In contrast, tidally flushed systems such as Ria de Aveiro and the Dutch Delta experience continuous microbial and DOM renewal through exchanges with coastal ocean. These site-specific contrasts indicate that differences in hydrological confinement and water exchange directly modulate DOM reactivity and turnover, thereby conditioning carbon mineralization pathways and associated GHG emissions. Several studies demonstrate how the interplay between catchment-scale and in-lake processes shapes DOM quality and lability, subsequently influencing carbon processing and greenhouse gas (GHG) emissions (Raymond and Bauer, 2000, He et al., 2022; Valiente et al., 2022; Cui et al., 2024).

4. Conclusions

This study reveals marked variability in DOM concentration and optical properties across European coastal wetlands, largely driven by hydrological regime and climatic conditions. Mediterranean systems show the highest DOM concentrations as a result of evaporative stress and hydrological confinement, whereas northern and Atlantic tidal wetlands exhibit low and less variable values since strong diel water fluxes drive DOM runoff, albeit with discernible differences among systems (Ria de Aveiro and Dutch DeltaThe Netherlands). Seasonality and ecological conditions introduce secondary but detectable sources of variability.

This study provides an initial framework to understand, at European scale, how hydrological management and restoration can modulate carbon retention and transformation in coastal wetlands. DOM emerges as a sensitive indicator of wetland functioning and a practical tool for guiding restoration toward improved carbon sequestration. Incorporating DOM concentration and optical properties, such as SUVA, fluorescence components and spectral slopes, into monitoring programs would allow early detection of shifts in carbon cycling pathways and strengthen climate-mitigation strategies.

As the first European-scale assessment of DOM dynamics in coastal wetlands, this work establishes a baseline to evaluate future changes. Under emerging climate scenarios, marked by rising temperatures, sea-level rise, enhanced evaporative stress and altered precipitation patterns, existing differences in DOM concentration and quality are expected to intensify, reinforcing divergent trajectories among confined, transitional and tidally influenced wetlands. However, predicting the fate of this C requires coupling DOM concentration and optical properties with biological lability, to reveal whether this C pool is likely to be retained over the long-term storage or rapidly mineralized. In this context, integrating lateral carbon transport with DOM transformation pathways, including its conversion into GHG, will be essential to better assess the role of coastal wetlands in regional and global carbon fluxes.

Data availability

Data, as well as related metadata, presented in this article will be deposited shortly at LifeWatch ERIC (https://data.lifewatchitaly.eu/) and will be fully accessible after December 31st, 2027. During embargo period, data will be made available upon reasonable request.

Author contributions

Conceptualization: CS, CR, AC. Investigation: CS, CT, GC, MG, MC, SV, VE, GB, AC. Formal analyses CR, JS, PB. Visualization JS, CT. Data curator: CT, GC, MG, MC, SV, VE, GB, LIW, PC, DK, SR. Resources: AC, AB, BO, CM, BM, DM, AP, ACS, JMP, MJY, MCB, LC, RC, MP, MvP, MB, JP, DV, WS, NB, MA, VD, RG, TR, SH, JG, ET, MK, RA, AG, RL, KA, PC, SR, AS, CC, LIW, MR. Project administration: AL, AC. CS and CR prepared the original draft, that was revised by all co-authors, AC revised the final version.

Competing interests

The authors declare that they have no conflict of interest.

Acknowledgements

This research has received funding from the project RESTORE4Cs - Modelling RESTORation of wEtlands for Carbon pathways, Climate Change mitigation and adaptation, ecosystem services, and biodiversity, Co-benefits (DOI: 10.3030/101056782), co-funded by the European Union under the Horizon Europe research and innovation programme (Grant Agreement ID: 101056782). The views and opinions expressed are those of the author(s) only and do not necessarily reflect those of the European Union or the granting authority. Neither the European Union nor the granting authority can be held responsible for them. UAveiro team acknowledge the support of CESAM-Centro de Estudos do Ambiente e do Mar, funded by national funds through FCT - Fundação para a Ciência e a Tecnologia I.P., under the project references UID/50017/2025 (doi.org/10.54499/UID/50017/2025) and LA/P/0094/2020 (doi.org/10.54499/LA/P/0094/2020). Work by the University of Valencia was also co-supported by projects CLIMAWET-CONS (PID2019-104742RB-I00), funded by the Agencia Estatal de Investigación of the Spanish Government, and by the project ECCAEL (PROMETEO CIPROM-2023-031), funded by the Generalitat Valenciana, both granted to Antonio Camacho.

695

References

Amaral, V., Ortega, T., Romera-Castillo, C., and Forja, J.: Linkages between greenhouse gases (CO2, CH4, and N2O) and dissolved organic matter composition in a shallow estuary, Sci. Total Environ., 788, 147863, https://doi.org/10.1016/j.scitotenv.2021.147863, 2021.

700 Angelotti de Ponte Rodrigues, N., Carmigniani, R., Guillot-Le Goff, A., Lucas, F. S., Therial, C., Naloufi, M., Janne, A., Piccioni, F., Saad, M., Dubois, P., and Vinçon-Leite, B.: Fluorescence spectroscopy for tracking microbiological contamination in urban waterbodies, Frontiers in Water, 6, https://doi.org/10.3389/frwa.2024.1358483, 2024.

Asmala, E., Autio, R., Kaartokallio, H., Stedmon, C. A., and Thomas, D. N.: Processing of humic-rich riverine dissolved organic matter by estuarine bacteria: Effects of predegradation and inorganic nutrients, Aquat Sci, 76, 451–463,

705 https://doi.org/10.1007/s00027-014-0346-7, 2014.

Bachi, G., Morelli, E., Gonnelli, M., Balestra, C., Casotti, R., Evangelista, V., Repeta, D. J., and Santinelli, C.: Fluorescent properties of marine phytoplankton exudates and lability to marine heterotrophic prokaryotes degradation, Limnol Oceanogr, 68, 982–1000, https://doi.org/10.1002/lno.12325, 2023.

Batista-Andrade, J. A., Diaz, E., Iglesias Vega, D., Hain, E., Rose, M. R., and Blaney, L.: Spatiotemporal analysis of

710 fluorescent dissolved organic matter to identify the impacts of failing sewer infrastructure in urban streams, Water Res, 229, 119521, https://doi.org/10.1016/j.watres.2022.119521, 2023.

Borisover, M., Laor, Y., Parparov, A., Bukhanovsky, N., and Lado, M.: Spatial and seasonal patterns of fluorescent organic matter in Lake Kinneret (Sea of Galilee) and its catchment basin, Water Res, 43, 3104–3116, https://doi.org/10.1016/j.watres.2009.04.039, 2009.

715 Butturini, A., Herzsprung, P., Lechtenfeld, O., et al.. Origin, accumulation and fate of dissolved organic matter in an extreme hypersaline shallow lake. Water Res. 118727, 2022.

Catalá, T.S., Reche, I., Álvarez, M., Khatiwala, S., Guallart, E.F., Benítez-Barrios, V.M., Fuentes-Lema, A., Romera-Castillo, C., Nieto-Cid, M., Pelejero, C., Fraile-Nuez, E., Ortega-Retuerta, E., Marrasé, C., Álvarez-Salgado, X.A.: Water mass age and aging driving chromophoric dissolved organic matter in the dark global ocean, Global Biogeochem. Cycles, 29, 917–934.

720 https://doi.org/10.1002/2014GB005048, 2015.

Chiasson-Gould, S. A., Blais, J. M., and Poulain, A. J.: Dissolved Organic Matter Kinetically Controls Mercury Bioavailability to Bacteria, Environ Sci Technol, 48, 3153–3161, https://doi.org/10.1021/es4038484, 2014.

Chupakov, A. V., Neverova, N. V., Chupakova, A. A., Zabelina, S. A., Shirokova, L. S., Vorobyeva, T. Y., and Pokrovsky, O. S.: Seasonal and spatial pattern of dissolved organic matter biodegradation and photodegradation in boreal humic waters,

725 Biogeosciences, 21, 5725–5743, https://doi.org/10.5194/bg-21-5725-2024, 2024.

Coble, P.G.: Characterization of marine and terrestrial DOM in seawater using excitation-emission matrix spectroscopy. Mar. Chem. 51, 325–346. https://doi.org/10.1016/0304-4203(95)00062-3, 1996.

Coplen, T. B. and Wassenaar, L. I.: LIMS for Lasers 2015 for achieving long-term accuracy and precision of δ 2 H, δ 17 O, and δ 18 O of waters using laser absorption spectrometry, Rapid Communications in Mass Spectrometry, 29, 2122–2130, https://doi.org/10.1002/rcm.7372, 2015.

Corrales-González, M., Rochera, C., Picazo, A., Camacho, A.: Trophic status and metabolic rates of threatened shallow saline lakes in Central Spain: Providing diagnostic elements for improving management strategies, Water Research, 270. https://doi.org/10.1016/j.watres.2024.122830, 2025.

Cory, R. M., Harrold, K. H., Neilson, B. T., and Kling, G. W.: Controls on dissolved organic matter (DOM) degradation in a headwater stream: The influence of photochemical and hydrological conditions in determining light-limitation or substrate-limitation of photo-degradation, Biogeosciences, 12, 6669–6685, https://doi.org/10.5194/bg-12-6669-2015, 2015.

Cui, S., Liu, P., Guo, H., Nielsen, C.K., Pullens, J.W.M., Chen, Q., Pugliese, L., Wu, S.: Wetland hydrological dynamics and methane emissions. Commun Earth Environ 5, 470. https://doi.org/10.1038/s43247-024-01635-w, 2024.

Deininger, A. and Frigstad, H.: Reevaluating the role of organic matter sources for coastal eutrophication, oligotrophication and ecosystem health, Front Mar Sci, 6, 210, https://doi.org/10.3389/fmars.2019.00210, 2019.

Del Vecchio, R. and Blough, N. V.: On the origin of the optical properties of humic substances. Environ. Sci. Technol. 38, 3885–3891, 2004.

Elsey-Quirk, T., Graham, S. A., Mendelssohn, I. A., Snedden, G., Day, J. W., Twilley, R. R., Shaffer, G., Sharp, L. A., Pahl, J., and Lane, R. R.: Mississippi river sediment diversions and coastal wetland sustainability: Synthesis of responses to freshwater, sediment, and nutrient inputs, Estuar Coast Shelf Sci, 221, 170–183, https://doi.org/10.1016/j.ecss.2019.03.002, 2019.

Fichot, C. G. and Benner, R.: The spectral slope coefficient of chromophoric dissolved organic matter (S 275-295) as a tracer of terrigenous dissolved organic carbon in river-influenced ocean margins , Limnol Oceanogr, 57, 1453–1466, https://doi.org/10.4319/lo.2012.57.5.1453, 2012.

Fluet-Chouinard, E., Stocker, B. D., Zhang, Z., Malhotra, A., Melton, J. R., Poulter, B., Kaplan, J. O., Goldewijk, K. K., Siebert, S., Minayeva, T., Hugelius, G., Joosten, H., Barthelmes, A., Prigent, C., Aires, F., Hoyt, A. M., Davidson, N., Finlayson, C. M., Lehner, B., Jackson, R. B., and McIntyre, P. B.: Extensive global wetland loss over the past three centuries, Nature, 614, 281–286, https://doi.org/10.1038/s41586-022-05572-6, 2023.

Fukushima, T., Park, J., Imai, A., and Matsushige, K.: Dissolved organic carbon in a eutrophic lake; dynamics, biodegradability and origin, Aquat Sci, 58, 139–157, https://doi.org/10.1007/BF00877112, 1996.

Galletti, Y., Gonnelli, M., Retelletti, S.B., Vestri, S., Santinelli, C.: DOM dynamics in open waters of the Mediterranean Sea: New insights from optical properties. Deep Sea Res. Part I Oceanogr. Res. Pap. https://doi.org/10.1016/j.dsr.2019.01.007, 2019.

García, P. E., Mansilla Ferro, C. F., and Diéguez, M. C.: Characterisation of dissolved organic matter from temperate wetlands: field dynamics and photoreactivity changes driven by natural inputs and diagenesis along the hydroperiod, N Z J Mar Freshwater Res, 57, 480–494, https://doi.org/10.1080/00288330.2022.2064882, 2022.

Goranov, A. I., Swinton, M. W., Winkler, D. A., Farrell, J. L., Nierzwicki-Bauer, S. A., and Wagner, S.: Assessing the spatiotemporal variability of dissolved organic matter fluorescence composition in the Lake George, NY watershed, Biogeochemistry, 167, 849–870, https://doi.org/10.1007/s10533-024-01147-x, 2024.

Graeber, D., Gelbrecht, J., Pusch, M. T., Anlanger, C., and von Schiller, D.: Agriculture has changed the amount and composition of dissolved organic matter in Central European headwater streams, Sci. Total Environ., 438, 435–446, https://doi.org/10.1016/j.scitotenv.2012.08.087, 2012.

Grasset, C., Einarsdottir, K., Catalán, N., Tranvik, L. J., Groeneveld, M., Hawkes, J. A., Attermeyer, K.: Decreasing photoreactivity and concurrent change in dissolved organic matter composition with increasing inland water residence time. Global Biogeochemical Cycles, 38, e2023GB007989. https://doi.org/10.1029/2023GB007989, 2024.

Gullian-Klanian, M., Gold-Bouchot, G., Delgadillo-Díaz, M., Aranda, J., and José Sánchez-Solís, M.: Effect of the use of Bacillus spp. on the characteristics of dissolved fluorescent organic matter and the phytochemical quality of Stevia rebaudiana grown in a recirculating aquaponic system, Environ Sci Pollut Res Int, 28, 36326–36343, https://doi.org/10.1007/s11356-021-13148-6, 2021.

Häder, D. P., Williamson, C. E., Wängberg, S. Å., Rautio, M., Rose, K. C., Gao, K., Helbling, E. W., Sinha, R. P., and Worrest, R.: Effects of UV radiation on aquatic ecosystems and interactions with other environmental factors, Photochemical and Photobiological Sciences, 14, 108–126, https://doi.org/10.1039/c4pp90035a, 2015.

Häder, D.-P. and Barnes, P. W.: Comparing the impacts of climate change on the responses and linkages between terrestrial and aquatic ecosystems, Sci. Total Environ., 682, 239–246, https://doi.org/10.1016/j.scitotenv.2019.05.024, 2019.

Hansell, D.A.: Dissolved organic carbon reference material program. EosTrans. Am. Geophys. Union 86, 318. https://doi.org/10.1029/2004GL020684.w, 2005.

Hansell, D.A. and Carlson, C.A.: Localized refractory dissolved organic carbon sinks in the deep ocean. Global Biogeochem. Cycles 27, 705–710. https://doi.org/10.1002/gbc.20067, 2013.

He, F., Ma, J., Lai, Q., Pei, D., & Li, W.: Association between greenhouse gases and dissolved organic matter composition in the main rivers around Taihu Lake. Journal of Freshwater Ecology, 37(1), 467–479. https://doi.org/10.1080/02705060.2022.2108924, 2022.

Helms, J. R., Stubbins, A., Ritchie, J. D., Minor, E. C., Kieber, D. J., and Mopper, K.: Absorption spectral slopes and slope ratios as indicators of molecular weight, source, and photobleaching of chromophoric dissolved organic matter, Limnol Oceanogr, 53, 955–969, https://doi.org/10.4319/lo.2008.53.3.0955, 2008.

Herbert, E. R., Boon, P., Burgin, A. J., Neubauer, S. C., Franklin, R. B., Ardon, M., Hopfensperger, K. N., Lamers, L. P. M., Gell, P., and Langley, J. A.: A global perspective on wetland salinization: Ecological consequences of a growing threat to freshwater wetlands, Ecosphere, 6, https://doi.org/10.1890/ES14-00534.1, 2015.

Hessen, D. O.: Dissolved organic carbon in a humic lake: effects on bacterial production and respiration, Hydrobiologia, 229, 115–123, https://doi.org/10.1007/BF00006995, 1992.

Kalbitz, K., Schwesig, D., Rethemeyer, J., Matzner, E.: Stabilization of dissolved organic matter by sorption to the mineral soil. Soil Biology and Biochemistry. 37, 7, 1319-1331. https://doi.org/10.1016/j.soilbio.2004.11.028, 2005.

Kinsey, J.D., Corradino, G., Ziervogel, K., Schnetzer, A., Osburn, C.L.: Formation of Chromophoric Dissolved Organic Matter by Bacterial Degradation of Phytoplankton-Derived Aggregates. Front. Mar. Sci. 4:430. doi: 10.3389/fmars.2017.00430, 2018.

Kurek, M. R., Frey, K. E., Guillemette, F., Podgorski, D. C., Townsend-Small, A., Arp, C. D., Kellerman, A. M., and Spencer, R. G. M.: Trapped Under Ice: Spatial and Seasonal Dynamics of Dissolved Organic Matter Composition in Tundra Lakes, J Geophys Res Biogeosci, 127, https://doi.org/10.1029/2021JG006578, 2022.

Kurek, M. R., Wickland, K. P., Nichols, N. A., McKenna, A. M., Anderson, S. M., Dornblaser, M. M., Koupaei-Abyazani, N., Poulin, B. A., Bansal, S., Fellman, J. B., Druschel, G. K., Bernhardt, E. S., and Spencer, R. G. M.: Linking Dissolved Organic Matter Composition to Landscape Properties in Wetlands Across the United States of America, Global Biogeochem Cycles, 38, https://doi.org/10.1029/2023GB007917, 2024.

Lambert, T., Pierson-Wickmann, A-C., Gruau, G., Jaffrézic, A., Petitjean, P., Thibault, J-N., Jeanneau, L.: DOC sources and DOC transport pathways in a small headwater catchment as revealed by carbon isotope fluctuation during storm events. Biogeosciences 11:3043–3056, 2014.

Lambert, T., Bouillon, S., Darchambeau, F., Morana, C., Roland, F. A. E., Descy, J. P., and Borges, A. V.: Effects of human land use on the terrestrial and aquatic sources of fluvial organic matter in a temperate river basin (The Meuse River, Belgium), Biogeochemistry, 136, 191–211, https://doi.org/10.1007/s10533-017-0387-9, 2017.

Lawaetz, A. J. and Stedmon, C. A.: Fluorescence Intensity Calibration Using the Raman Scatter Peak of Water, Appl Spectrosc, 63, 936–940, https://doi.org/10.1366/000370209788964548, 2009.

Logozzo, L. A., Hosen, J. D., McArthur, J., and Raymond, P. A.: Distinct drivers of two size fractions of operationally dissolved iron in a temperate river, Limnol Oceanogr, 68, 1185–1200, https://doi.org/10.1002/lno.12338, 2023.

Lorenzen, C.J.: Determination of chlorophyll and phaeopigments: spectrophotometric equations. Limnol. Oceanogr. 12, 343-346. https://doi.org/10.4319/lo.1967.12.2.0343., 1967.

Marcé, R., Verdura, L., and Leung, N.: Dissolved organic matter spectroscopy reveals a hot spot of organic matter changes at the river–reservoir boundary, Aquat Sci, 83, https://doi.org/10.1007/s00027-021-00823-6, 2021.

Misteli, B., Morant, D., Camacho, A., Adamo, M., Bachi, G., Bègue, N., Bučas, M., Cabrera-Brufau, M., Carballeira, R., Cavalcante, L., Cazacu, C., Coelho, J., Doebke, C., Dinu, V., Guelmami, A., Giuca, R., Kataržytė, M., Lillebø, A., Marin, A., Marangi, C., Minaudo, C., Montes-Pérez, J., Obrador, B., Oliveira, B., Petkuvienė, J., Picazo, A., van Puijenbroek, M., Ronse, M., Rochera, C., Sánchez, A., Santinelli, C., Sousa, A., von Schiller, D., Attermeyer, K., Tropea, C., and Vaičiūtė, D.: Coastal Wetland Restoration and Greenhouse Gas Pathways: A Global Meta-Analysis, EarthArXiv[preprint], https://doi.org/10.31223/X51B39, 14 November 2025.

Mitsch, W. J., Bernal, B., and Hernandez, M. E.: Ecosystem services of wetlands, Int J Biodivers Sci Ecosyst Serv Manag, 11, 1–4, https://doi.org/10.1080/21513732.2015.1006250, 2015.

Murphy, K. R., Stedmon, C. A., Graeber, D., and Bro, R.: Fluorescence spectroscopy and multi-way techniques. PARAFAC, Analytical Methods, 5, 6557, https://doi.org/10.1039/c3ay41160e, 2013.

Murphy, K. R., Stedmon, C. A., Wenig, P., and Bro, R.: OpenFluor– an online spectral library of auto-fluorescence by organic compounds in the environment, Anal. Methods, 6, 658–661, https://doi.org/10.1039/C3AY41935E, 2014.

Oliveira, R.B., Camacho, A., Guelmami, A., Schroder, C., Bègue, N., Bučas, M., Cazacu, C., Ciravegna, E., Coelho, J.P., Relu Giuca, C., Hilaire, S., Kataržytė, M., Morant, D., Picazo, A., Polman, N., van Puijenbroek, M., Raoult, J., Rochera, C., Ronse, M., Lillebø, A. I.: European coastal wetlands datasets and their use in decision-support tools for policy restoration objectives. Environmental Science and Policy (under review).

Omanović, D., Marcinek, S., and Santinelli, C.: TreatEEM - A Software Tool for the Interpretation of Fluorescence Excitation-Emission Matrices (EEMs) of Dissolved Organic Matter in Natural Waters, Water (Basel), 15, 2214, https://doi.org/10.3390/w15122214, 2023.

Omanović, D., Santinelli, C., Marcinek, S., and Gonnelli, M.: ASFit - An all-inclusive tool for analysis of UV–Vis spectra of colored dissolved organic matter (CDOM), Comput Geosci, 133, 104334, https://doi.org/10.1016/j.cageo.2019.104334, 2019.

Orlova, J., Amiri, F., Bourgeois, A. K., Buttle, J. M., Cherlet, E., Cuss, C. W., Devito, K. J., Emelko, M. B., Floyd, W. C., Foster, D. E., Hutchins, R. H. S., Jamieson, R., Johnson, M. S., McSorley, H. J., Silins, U., Tank, S. E., Thompson, L. M., Webster, K. L., Williams, C. H. S., and Olefeldt, D.: Composition of Stream Dissolved Organic Matter Across Canadian Forested Ecozones Varies in Three Dimensions Linked to Landscape and Climate, Water Resour Res, 60, https://doi.org/10.1029/2023WR035196, 2024.

Ouyang, T., McKenna, A. M., and Wozniak, A. S.: Storm-driven hydrological, seasonal, and land use/land cover impact on dissolved organic matter dynamics in a mid-Atlantic, USA coastal plain river system characterized by 21 T FT-ICR mass spectrometry, Front Environ Sci, 12, https://doi.org/10.3389/fenvs.2024.1379238, 2024.

Peleato, N. M., McKie, M., Taylor-Edmonds, L., Andrews, S. A., Legge, R. L., and Andrews, R. C.: Fluorescence spectroscopy for monitoring reduction of natural organic matter and halogenated furanone precursors by biofiltration, Chemosphere, 153, 155–161, https://doi.org/10.1016/j.chemosphere.2016.03.018, 2016.

Peleato, N. M., Sidhu, B. S., Legge, R. L., and Andrews, R. C.: Investigation of ozone and peroxone impacts on natural organic matter character and biofiltration performance using fluorescence spectroscopy, Chemosphere, 172, 225–233, https://doi.org/10.1016/j.chemosphere.2016.12.118, 2017.

Pillai, K.C.S.: Some New Test Criteria in Multivariate Analysis. Ann. Math. Statist. 26 (1) 117 - 121, March, 1955. https://doi.org/10.1214/aoms/1177728599, 1955.

Raymond, P.A., Bauer, J.E.: Bacterial consumption of DOC during transport through a temperate estuary. Aquat Microb Ecol 22:1-12 https://doi.org/10.3354/ame022001, 2000

Regulation (EU) 2024/1991 of the European Parliament and of the Council of 24 June 2024 on nature restoration and amending Regulation (EU) 2022/869. (2024). Official Journal of the European Union, L, 2024/1991. http://data.europa.eu/eli/reg/2024/1991/oj

Retelletti Brogi, S., Balestra, C., Casotti, R., Cossarini, G., Galletti, Y., Gonnelli, M., Vestri, S., Santinelli, C.: Time resolved data unveils the complex DOM dynamics in a Mediterranean river. Sci. Total Environ. 733, 139212. https://doi.org/10.1016/J.SCITOTENV.2020.139212, 2020.

Retelletti Brogi, S., Casotti, R., Misson, B., Balestra, C., Gonnelli, M., Vestri, S., Santinelli, C.: DOM Biological Lability in an Estuarine System in Two Contrasting Periods. J. Mar. Sci. Eng. 2021, Vol. 9, Page 172 9, 172. https://doi.org/10.3390/JMSE9020172, 2021.

Retelletti Brogi, S., Gonnelli, M., Vestri, S., and Santinelli, C.: Biophysical processes affecting DOM dynamics at the Arno river mouth (Tyrrhenian Sea), Biophys Chem, 197, 1–9, https://doi.org/10.1016/j.bpc.2014.10.004, 2015.

Robertson, H., Fennessy, S., Hilton, G., Job, N., Kumar, R., Simpson, M., Aggestam, F., Aldred, M., Chacón, A., Costanza, R., Davidson, N., Field, C., Finlayson, C. M., Gandra, F., Gillis, L. G., Hernández-Blanco, M., Moritsch, M., Thornton, S., Wood, K., & van 't Hoff, V. (2025). Global Wetland Outlook 2025: Valuing, conserving, restoring and financing wetlands. https://doi.org/10.69556/GWO-2025-eng

Rochera, C., Peña, M., Picazo, A., Morant, D., Miralles-Lorenzo, J., Camacho-Santamans, A., Belenguer-Manzanedo, M., Montoya, T., Fayos, G., and Camacho, A.: Naturalization of treated wastewater by a constructed wetland in a water-scarce Mediterranean region, J Environ Manage, 357, 120715, https://doi.org/10.1016/j.jenvman.2024.120715, 2024.

Romera-Castillo, C., Sarmento, H., Alvarez-Salgado, X.A., Gasol, J.M., Marrasé, C.: Net production and consumption of fluorescent colored dissolved organic matter by natural bacterial assemblages growing on marine phytoplankton exudates. Appl. Environ. Microbiol. 77, 7490–8. https://doi.org/10.1128/AEM.00200-11, 2011.

Santinelli, C.: DOC in the Mediterranean Sea. Academic Press. https://doi.org/10.1016/B978-0-12-405940-5.00013-3, 2015

Santinelli, C., Follett, C., Retelletti Brogi, S., Xu, L., Repeta, D.: Carbon isotope measurements reveal unexpected cycling of dissolved organic matter in the deep Mediterranean Sea. Mar. Chem. 177. https://doi.org/10.1016/j.marchem.2015.06.018, 2015.

Shang, P., Lu, Y., Du, Y., Jaffé, R., Findlay, R. H., and Wynn, A.: Climatic and watershed controls of dissolved organic matter variation in streams across a gradient of agricultural land use, Sci. Total Environ., 612, 1442–1453, https://doi.org/10.1016/j.scitotenv.2017.08.322, 2018.

Singh, S., Inamdar, S., Mitchell, M., and McHale, P.: Seasonal pattern of dissolved organic matter (DOM) in watershed sources: Influence of hydrologic flow paths and autumn leaf fall, Biogeochemistry, 118, 321–337, https://doi.org/10.1007/s10533-013-9934-1, 2014.

Stedmon, C., Markager, S.: Resolving the variability of dissolved organic matter fluorescence in a temperate estuary and its catchment using PARAFAC analysis. Limnol. Oceanogr. 50, 686–697. https://doi.org/10.4319/lo.2005.50.2.0686, 2005.

Thibault, A., Derenne, S., Parlanti, E., Anquetil, C., Sourzac, M., Budzinski, H., Fuster, L., Laverman, A., Roose-Amsaleg, C., Viollier, E., Huguet, A.: Dynamics of organic matter in the Seine Estuary (France): Bulk and structural approaches. Mar. Chem. 212, 108–119. https://doi.org/10.1016/J.MARCHEM.2019.04.007, 2019.

Vähätalo, A. V. and Wetzel, R. G.: Long-term photochemical and microbial decomposition of wetland-derived dissolved organic matter with alteration of 13C:12C mass ratio, Limnol Oceanogr, 53, 1387–1392, https://doi.org/10.4319/lo.2008.53.4.1387, 2008.

Valiente, N., Eiler, A., Allesson, L., Andersen, T., Clayer, F., Crapart, C., Dörsch, P., Fontaine, L., Heuschele, J., Vogt, R.D., Wei, J., de Wit, H.A., Hessen, D.O.: Catchment properties as predictors of greenhouse gas concentrations across a gradient of boreal lakes. Front. Environ. Sci. 10:880619. doi: 10.3389/fenvs.2022.880619, 2022.

Van Asselen, S., Verburg, P. H., Vermaat, J. E., and Janse, J. H.: Drivers of wetland conversion: A global meta-analysis, PLoS One, 8, https://doi.org/10.1371/journal.pone.0081292, 2013.

Voss, M., Asmala, E., Bartl, I., Carstensen, J., Conley, D. J., Dippner, J. W., Humborg, C., Lukkari, K., Petkuviene, J., Reader, H., Stedmon, C., Vybernaite-Lubiene, I., Wannicke, N., and Zilius, M.: Origin and fate of dissolved organic matter in four shallow Baltic Sea estuaries, Biogeochemistry, 154, 385–403, https://doi.org/10.1007/s10533-020-00703-5, 2021.

Wauthy, M., Rautio, M., Christoffersen, K. S., Forsström, L., Laurion, I., Mariash, H. L., Peura, S., and Vincent, W. F.: Increasing dominance of terrigenous organic matter in circumpolar freshwaters due to permafrost thaw, Limnol Oceanogr Lett, 3, 186–198, https://doi.org/10.1002/lol2.10063, 2018.

Weishaar, J. L., Aiken, G. R., Bergamaschi, B. A., Fram, M. S., Fujii, R., and Mopper, K.: Evaluation of specific ultraviolet absorbance as an indicator of the chemical composition and reactivity of dissolved organic carbon, Environ Sci Technol, 37, 4702–4708, https://doi.org/10.1021/es030360x, 2003.

Wen, Z., Shang, Y., Song, K., Liu, G., Hou, J., Lyu, L., Tao, H., Li, S., He, C., Shi, Q., and He, D.: Composition of dissolved organic matter (DOM) in lakes responds to the trophic state and phytoplankton community succession, Water Res, 224, 119073, https://doi.org/10.1016/j.watres.2022.119073, 2022.

Williams, P. and Faber, P.: Salt marsh restoration experience in San Francisco Bay, Journal of Coastal Research SI, 27, 203–311, 2001.

Yamashita, Y., Nosaka, Y., Suzuki, K., Ogawa, H., Takahashi, K., Saito, H.: Photobleaching as a factor controlling spectral characteristics of chromophoric dissolved organic matter in open ocean. Biogeosciences 10, 7207–7217. https://doi.org/10.5194/BG-10-7207-2013, 2013

Yang, L., Chen, W., Zhuang, W. E., Cheng, Q., Li, W., Wang, H., Guo, W., Chen, C. T. A., and Liu, M.: Characterization and bioavailability of rainwater dissolved organic matter at the southeast coast of China using absorption spectroscopy and fluorescence EEM-PARAFAC, Estuar Coast Shelf Sci, 217, 45–55, https://doi.org/10.1016/j.ecss.2018.11.002, 2019.

Yao, J., Chen, Z., Ge, J., and Zhang, W.: Source-To-sink pathways of dissolved organic carbon in the river-estuary-ocean continuum: A modeling investigation, Biogeosciences, 21, 5435–5455, https://doi.org/10.5194/bg-21-5435-2024, 2024.

Zhang, X., Cao, F., Huang, Y., and Tang, J.: Variability of dissolved organic matter in two coastal wetlands along the Changjiang River Estuary: Responses to tidal cycles, seasons, and degradation processes, Sci. Total Environ., 807, https://doi.org/10.1016/j.scitotenv.2021.150993, 2022.

Zhou, Y., Martin, P., and Müller, M.: Composition and cycling of dissolved organic matter from tropical peatlands of coastal Sarawak, Borneo, revealed by fluorescence spectroscopy and parallel factor analysis, Biogeosciences, 16, 2733–2749, https://doi.org/10.5194/bg-16-2733-2019, 2019.

Zhuang, W. E., Chen, W., Cheng, Q., and Yang, L.: Assessing the priming effect of dissolved organic matter from typical sources using fluorescence EEMs-PARAFAC, Chemosphere, 264, https://doi.org/10.1016/j.chemosphere.2020.128600, 2021.

Supplementary material

This study	Description	Attribution (Tucker 0.98)	Reference
$C1_{t\text{-}hum}$ $\lambda_{Ex}/\lambda_{Em}$ = 340/440 nm	C1	Terrestrial humic-like	Wauthy et al., 201
	C1	Terrestrial humic-like	Goranov et al 2024
	C1	Terrestrial humic-like	Peleato et al., 2017
	C1	humic like	Yang et al., 2019
	C1	Terrestrial humic-like	Gullian-Klanian et al., 2021
$C2_{t\text{-}hum}$ $\lambda_{Ex}/\lambda_{Em}$ = 305/430 nm	C4	UVA humic-like	Marcé et al., 2021
	C1	Terrestrial humic-like	Angelotti de Ponte Rodrigues et al., 2024
	C2	Terrestrial humic-like	Kurek et al., 2022
	C1	Terrestrial humic-like	Lambert et al., 2017
$C3_{fulvic}$ $\lambda_{Ex}/\lambda_{Em}$ = 385/495 nm	C2	fulvic acid-like	Graeber et al., 2012
	C2	humic like	Zhuang et al., 2021
	C2	humic/fulvic acid-like	C2 Zhou et al., 2019
$C4_{microb\text{-}hum}$ $\lambda_{Ex}/\lambda_{Em}$ = 310/390 nm	C4	microbial humic like	Peleato et al, 2017
	C4	marine humic like	Zhou et al., 2019
	C3	microbial humic like	Orlova et al., 2024
	C2	microbial humic like	Ouyang et al., 2024
$C5_{trp}$ $\lambda_{Ex}/\lambda_{Em}$ = 280/350 nm	C5	protein like (trp)	Logozzo et al., 2023
	C3	protein like	Borisover et al., 2009
	C7	protein like (trp)	Stedmon and Markager, 2005
	C5	protein trp	Peleato et al, 2016

Table S1 Characterization of the 5 components of fluorescent dissolved organic matter (FDOM) individuated by PARAFAC taking into consideration all the samples collected at the 6 wetlands by comparison with literature.

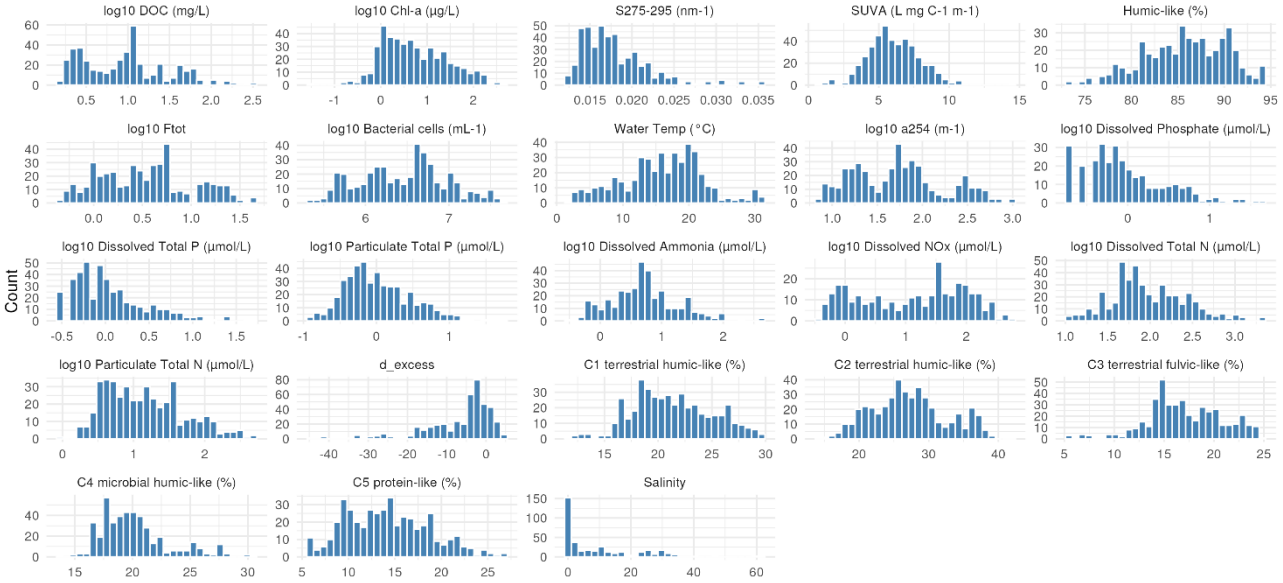

Figure S1: Distribution of environmental variables, DOC, CDOM and FDOM

960

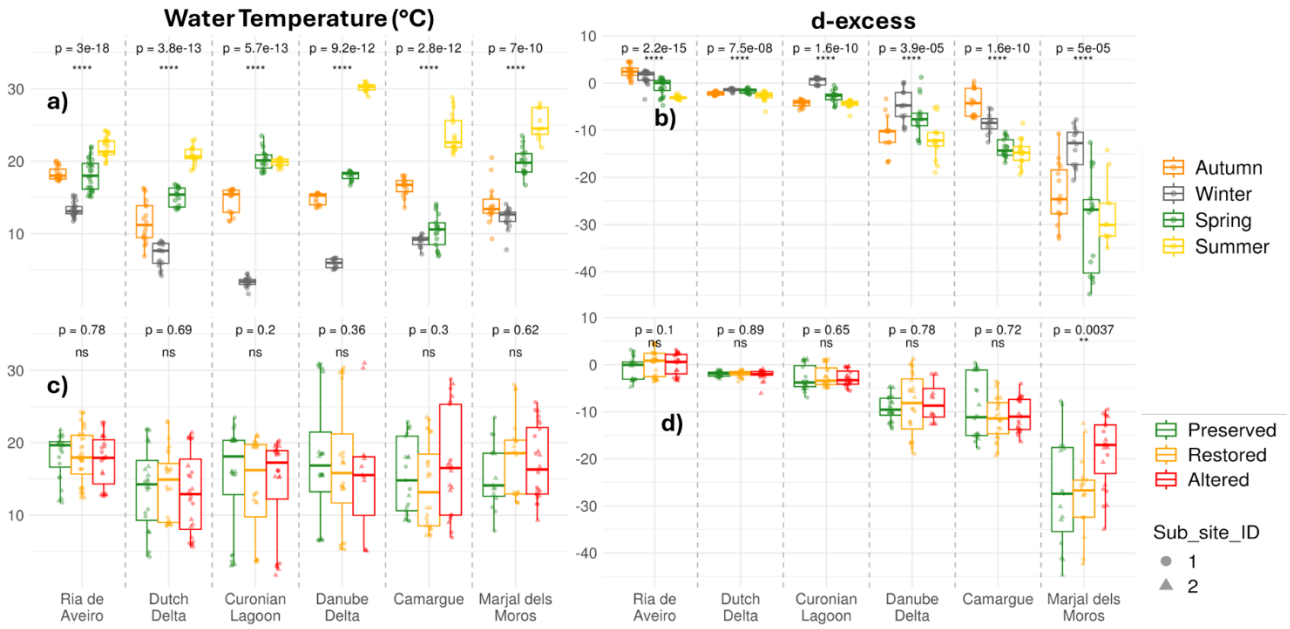

Figure S2. Boxplots of water temperature across the six studied European coastal wetlands, grouped by season (a) and ecological conditions (c) and d-excess across the six studied European coastal wetlands, grouped by season (b) and ecological conditions (d). Significant differences were assessed using the Kruskal–Wallis test. (*p<0.001, **p<0.01, *p<0.05, ns = no significance).**

965

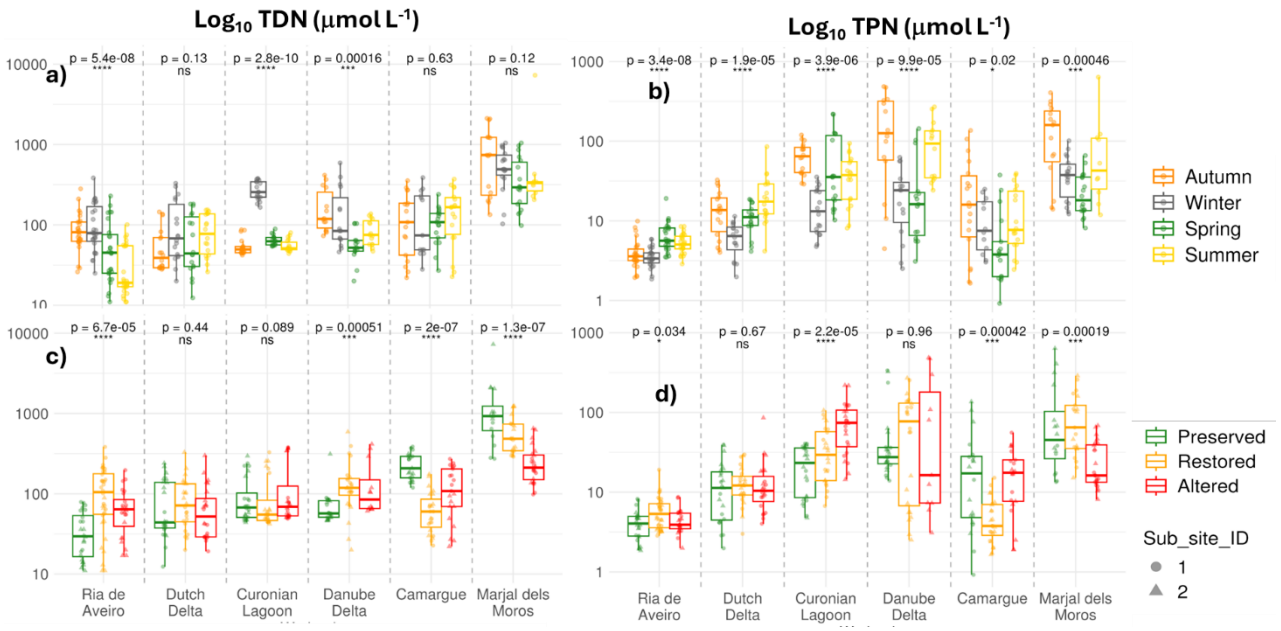

Figure S3. Boxplots of logarithmic scale of Total Dissolved Nitrogen (TDN) across the six studied European coastal wetlands, grouped by season (a) and ecological conditions (c) and logarithmic scale of Total Particulate Nitrogen (TDN) across the six studied European coastal wetlands, grouped by season (b) and ecological conditions (d). Significant differences were assessed using the Kruskal–Wallis test. (*p<0.001, **p<0.01, *p<0.05, ns = no significance).**

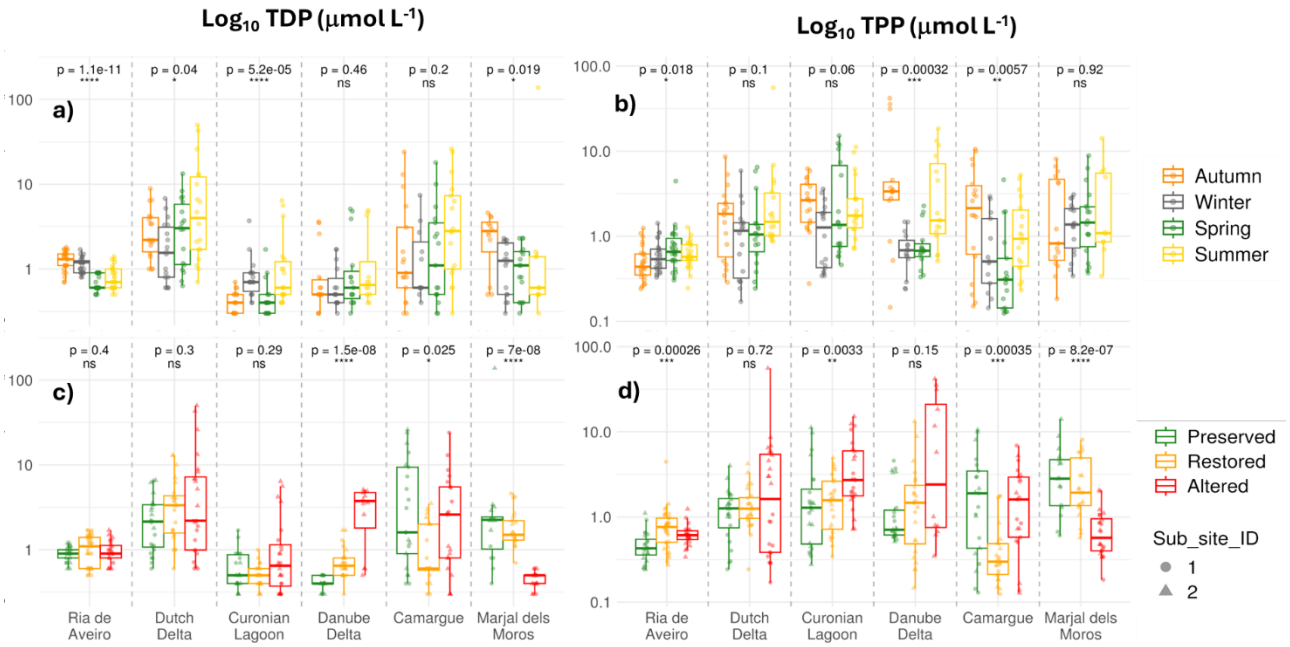

975

Figure S4. Boxplots of logarithmic scale of Total Dissolved Phosphorous (TDP) across the six studied European coastal wetlands, grouped by season (a) and ecological conditions (c) and logarithmic scale of Total Particulate Phosphorous (TDP) across the six studied European coastal wetlands, grouped by season (b) and ecological conditions (d). Significant differences were assessed using the Kruskal–Wallis test. (*p<0.001, **p<0.01, *p<0.05, ns = no significance).**

980

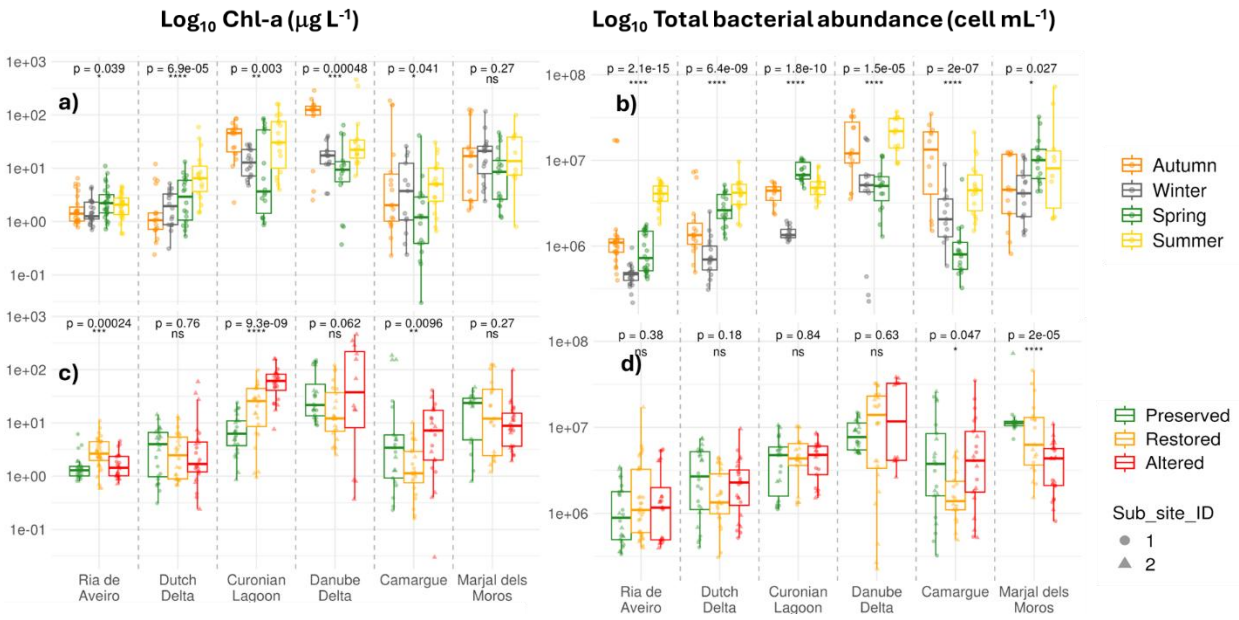

Figure S5. Boxplots of logarithmic scale of Total bacterial abundance across the six studied European coastal wetlands, grouped by season (a) and ecological conditions (c) and logarithmic scale of Chl-a across the six studied European coastal wetlands, grouped by season (b) and ecological conditions (d). Significant differences were assessed using the Kruskal–Wallis test. (*p<0.001, **p<0.01, *p<0.05, ns = no significance).**

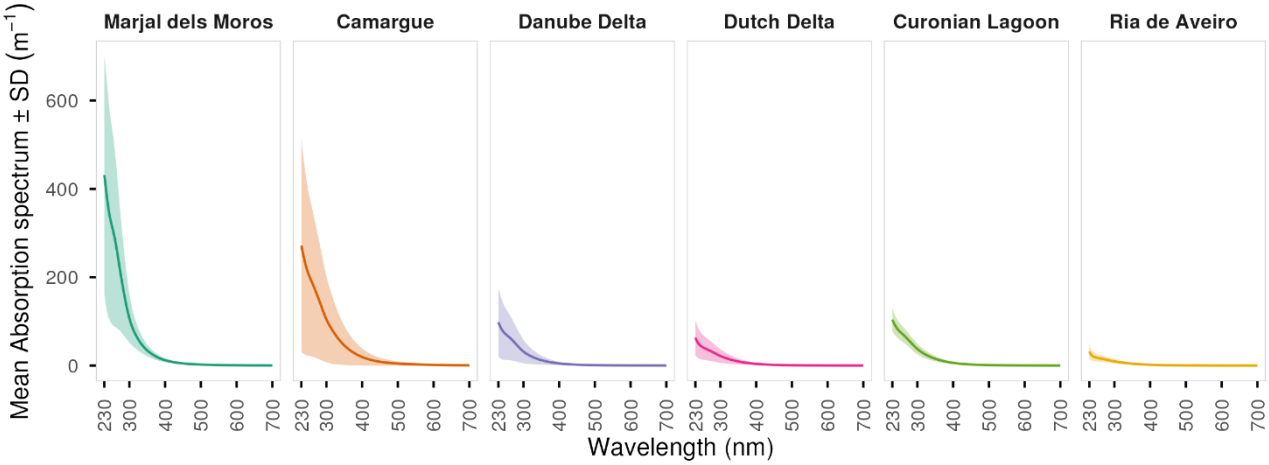

990 **Figure S6: Average spectra of absorption for each wetland. The shaded area represents the standard deviation across samples per wetland.**

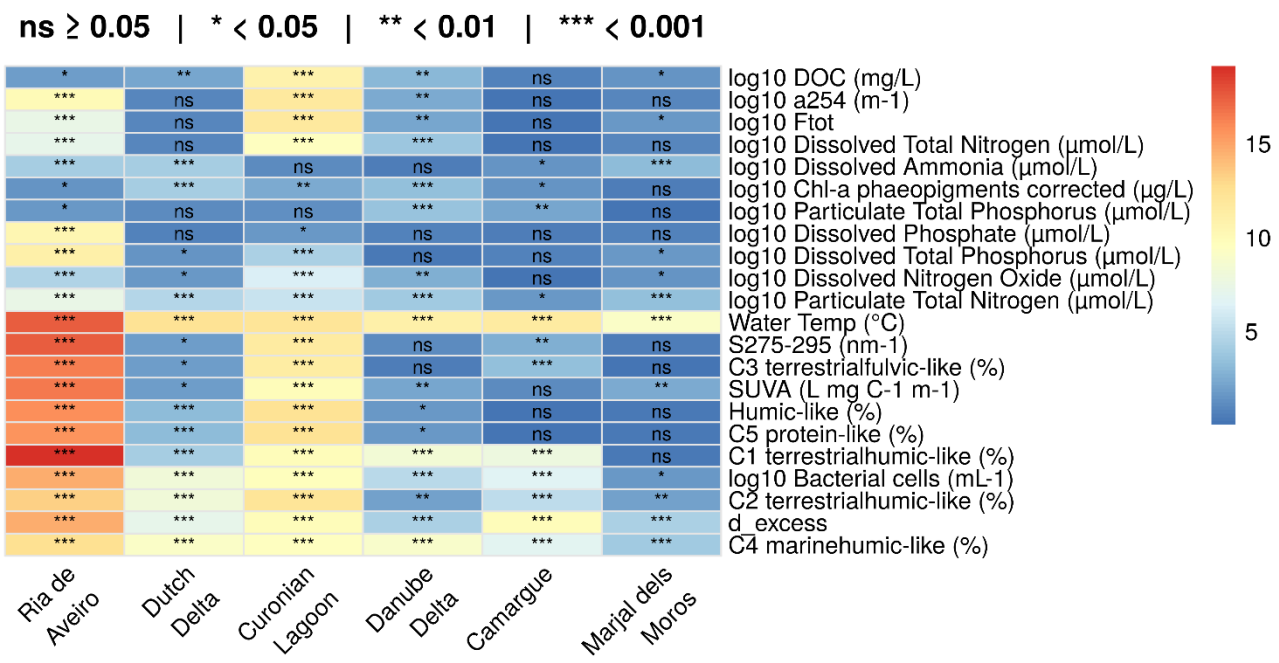

Figure S7: The heatmap shows the negative decadic logarithm of p values from Kruskal-Wallis tests assessing differences in the distribution of environmental parameters across seasons (Fig. S7) for each wetland. Text labels indicate significance thresholds: ns: not significant, p > 0.05; *, p < 0.05; **, p < 0.01; ***, p < 0.001.

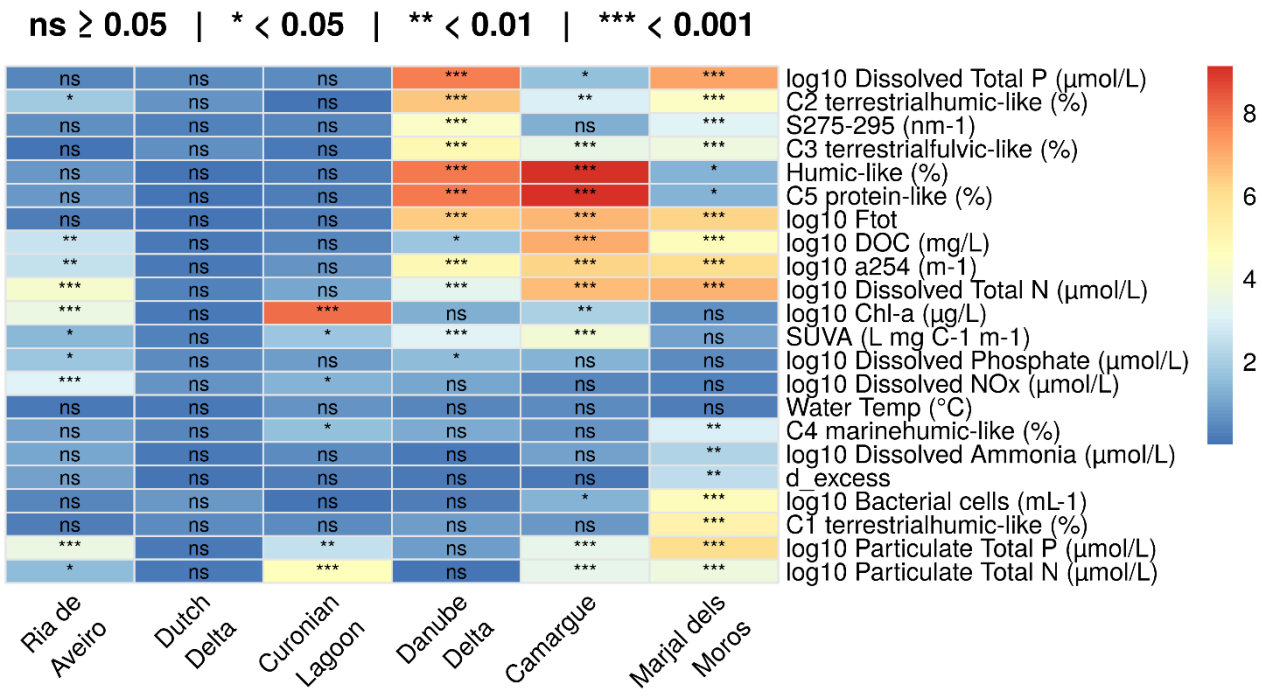

Figure S8: The heatmap shows the negative decadic logarithm of p values from Kruskal-Wallis tests assessing differences in the distribution of environmental parameters across ecological conditions (Fig. S8) for each wetland. Text labels indicate significance thresholds: ns: not significant, p > 0.05; *, p < 0.05; **, p < 0.01; ***, p < 0.001.

References

Angelotti de Ponte Rodrigues, N., Carmigniani, R., Guillot-Le Goff, A., Lucas, F. S., Therial, C., Naloufi, M., Janne, A., Piccioni, F., Saad, M., Dubois, P., and Vinçon-Leite, B.: Fluorescence spectroscopy for tracking microbiological contamination in urban waterbodies, Frontiers in Water, 6, https://doi.org/10.3389/frwa.2024.1358483, 2024.

Borisover, M., Laor, Y., Parparov, A., Bukhanovsky, N., and Lado, M.: Spatial and seasonal patterns of fluorescent organic matter in Lake Kinneret (Sea of Galilee) and its catchment basin, Water Res, 43, 3104–3116, https://doi.org/10.1016/j.watres.2009.04.039, 2009.

Goranov, A. I., Swinton, M. W., Winkler, D. A., Farrell, J. L., Nierzwicki-Bauer, S. A., and Wagner, S.: Assessing the spatiotemporal variability of dissolved organic matter fluorescence composition in the Lake George, NY watershed, Biogeochemistry, 167, 849–870, https://doi.org/10.1007/s10533-024-01147-x, 2024.

Graeber, D., Gelbrecht, J., Pusch, M. T., Anlanger, C., and von Schiller, D.: Agriculture has changed the amount and composition of dissolved organic matter in Central European headwater streams, Sci. Total Environ., 438, 435–446, https://doi.org/10.1016/j.scitotenv.2012.08.087, 2012.

Gullian-Klanian, M., Gold-Bouchot, G., Delgadillo-Díaz, M., Aranda, J., and José Sánchez-Solís, M.: Effect of the use of Bacillus spp. on the characteristics of dissolved fluorescent organic matter and the phytochemical quality of Stevia rebaudiana grown in a recirculating aquaponic system, Environ Sci Pollut Res Int, 28, 36326–36343, https://doi.org/10.1007/s11356-021-13148-6, 2021.

Kurek, M. R., Frey, K. E., Guillemette, F., Podgorski, D. C., Townsend-Small, A., Arp, C. D., Kellerman, A. M., and Spencer, R. G. M.: Trapped Under Ice: Spatial and Seasonal Dynamics of Dissolved Organic Matter Composition in Tundra Lakes, J Geophys Res Biogeosci, 127, https://doi.org/10.1029/2021JG006578, 2022.

Lambert, T., Bouillon, S., Darchambeau, F., Morana, C., Roland, F. A. E., Descy, J. P., and Borges, A. V.: Effects of human land use on the terrestrial and aquatic sources of fluvial organic matter in a temperate river basin (The Meuse River, Belgium), Biogeochemistry, 136, 191–211, https://doi.org/10.1007/s10533-017-0387-9, 2017.

Marcé, R., Verdura, L., and Leung, N.: Dissolved organic matter spectroscopy reveals a hot spot of organic matter changes at the river–reservoir boundary, Aquat Sci, 83, https://doi.org/10.1007/s00027-021-00823-6, 2021.

Orlova, J., Amiri, F., Bourgeois, A. K., Buttle, J. M., Cherlet, E., Cuss, C. W., Devito, K. J., Emelko, M. B., Floyd, W. C., Foster, D. E., Hutchins, R. H. S., Jamieson, R., Johnson, M. S., McSorley, H. J., Silins, U., Tank, S. E., Thompson, L. M., Webster, K. L., Williams, C. H. S., and Olefeldt, D.: Composition of Stream Dissolved Organic Matter Across Canadian Forested Ecozones Varies in Three Dimensions Linked to Landscape and Climate, Water Resour Res, 60, https://doi.org/10.1029/2023WR035196, 2024.

Ouyang, T., McKenna, A. M., and Wozniak, A. S.: Storm-driven hydrological, seasonal, and land use/land cover impact on dissolved organic matter dynamics in a mid-Atlantic, USA coastal plain river system characterized by 21 T FT-ICR mass spectrometry, Front Environ Sci, 12, https://doi.org/10.3389/fenvs.2024.1379238, 2024.

Peleato, N. M., McKie, M., Taylor-Edmonds, L., Andrews, S. A., Legge, R. L., and Andrews, R. C.: Fluorescence spectroscopy for monitoring reduction of natural organic matter and halogenated furanone precursors by biofiltration, Chemosphere, 153, 155–161, https://doi.org/10.1016/j.chemosphere.2016.03.018, 2016.

Peleato, N. M., Sidhu, B. S., Legge, R. L., and Andrews, R. C.: Investigation of ozone and peroxone impacts on natural organic matter character and biofiltration performance using fluorescence spectroscopy, Chemosphere, 172, 225–233, https://doi.org/10.1016/j.chemosphere.2016.12.118, 2017.

Yang, L., Chen, W., Zhuang, W. E., Cheng, Q., Li, W., Wang, H., Guo, W., Chen, C. T. A., and Liu, M.: Characterization and bioavailability of rainwater dissolved organic matter at the southeast coast of China using absorption spectroscopy and fluorescence EEM-PARAFAC, Estuar Coast Shelf Sci, 217, 45–55, https://doi.org/10.1016/j.ecss.2018.11.002, 2019.

Zhou, Y., Martin, P., and Müller, M.: Composition and cycling of dissolved organic matter from tropical peatlands of coastal Sarawak, Borneo, revealed by fluorescence spectroscopy and parallel factor analysis, Biogeosciences, 16, 2733–2749, https://doi.org/10.5194/bg-16-2733-2019, 2019.

Zhuang, W. E., Chen, W., Cheng, Q., and Yang, L.: Assessing the priming effect of dissolved organic matter from typical sources using fluorescence EEMs-PARAFAC, Chemosphere, 264, https://doi.org/10.1016/j.chemosphere.2020.128600, 2021.